Available online at www.sciencedirect.com
ScienceDirect
Geochimica et Cosmochimica Acta 72 (2008) 6177–6197
Geochimica et Cosmochimica Acta
www.elsevier.com/locate/gca

Hf–W mineral isochron for Ca,Al-rich inclusions: Age of the solar system and the timing of core formation in planetesimals

Christoph Burkhardt [a,b,*], Thorsten Kleine [a], Bernard Bourdon [a], Herbert Palme [b], Jutta Zipfel [c], Jon M. Friedrich [d], Denton S. Ebel [e]

[a] *Institute of Isotope Geochemistry and Mineral Resources, ETH Zurich, Clausiusstrasse 25, CH-8092 Zurich, Switzerland*
[b] *Institut für Geologie und Mineralogie, Universität zu Köln, Zülpicherstrasse 49b, D-50674 Köln, Germany*
[c] *Naturmuseum und Forschungsinstitut Senckenberg, Frankfurt, Germany*
[d] *Department of Chemistry, Fordham University, Bronx, NY 10458, USA*
[e] *Department of Earth and Planetary Sciences, The American Museum of Natural History, Central Park West at 79th Street, NY 10024-5192, USA*

Received 22 January 2008; accepted in revised form 29 October 2008; available online 5 November 2008

Abstract

Application of ^{182}Hf–^{182}W chronometry to constrain the duration of early solar system processes requires the precise knowledge of the initial Hf and W isotope compositions of the solar system. To determine these values, we investigated the Hf–W isotopic systematics of bulk samples and mineral separates from several Ca,Al-rich inclusions (CAIs) from the CV3 chondrites Allende and NWA 2364. Most of the investigated CAIs have relative proportions of ^{183}W, ^{184}W, and ^{186}W that are indistinguishable from those of bulk chondrites and the terrestrial standard. In contrast, one of the investigated Allende CAIs has a lower $^{184}W/^{183}W$ ratio, most likely reflecting an overabundance of *r*-process relative to *s*-process isotopes of W. All other bulk CAIs have similar $^{180}Hf/^{184}W$ and $^{182}W/^{184}W$ ratios that are elevated relative to average carbonaceous chondrites, probably reflecting Hf–W fractionation in the solar nebula within the first ~3 Myr. The limited spread in $^{180}Hf/^{184}W$ ratios among the bulk CAIs precludes determination of a CAI whole-rock isochron but the fassaites have high $^{180}Hf/^{184}W$ and radiogenic $^{182}W/^{184}W$ ratios up to ~14 ε units higher than the bulk rock. This makes it possible to obtain precise internal Hf–W isochrons for CAIs. There is evidence of disturbed Hf–W systematics in one of the CAIs but all other investigated CAIs show no detectable effects of parent body processes such as alteration and thermal metamorphism. Except for two fractions from one Allende CAI, all fractions from the investigated CAIs plot on a single well-defined isochron, which defines the initial $\varepsilon^{182}W = -3.28 \pm 0.12$ and $^{182}Hf/^{180}Hf = (9.72 \pm 0.44) \times 10^{-5}$ at the time of CAI formation. The initial $^{182}Hf/^{180}Hf$ and $^{26}Al/^{27}Al$ ratios of the angrites D'Orbigny and Sahara 99555 are consistent with the decay from initial abundances of ^{182}Hf and ^{26}Al as measured in CAIs, suggesting that these two nuclides were homogeneously distributed throughout the solar system. However, the uncertainties on the initial $^{182}Hf/^{180}Hf$ and $^{26}Al/^{27}Al$ ratios are too large to exclude that some ^{26}Al in CAIs was produced locally by particle irradiation close to an early active Sun. The initial $^{182}Hf/^{180}Hf$ of CAIs corresponds to an absolute age of 4568.3 ± 0.7 Ma, which may be defined as the age of the solar system. This age is 0.5–2 Myr older than the most precise ^{207}Pb–^{206}Pb age of Efremovka CAI 60, which does not seem to date CAI formation. Tungsten model ages for magmatic iron meteorites, calculated relative to the newly and more precisely defined initial $\varepsilon^{182}W$ of CAIs, indicate that core formation in their parent bodies occurred in less than ~1 Myr after CAI formation. This confirms earlier conclusions that the accretion of the parent bodies of magmatic iron meteorites predated chondrule formation and that their differentiation was triggered by heating from decay of abundant ^{26}Al. A more precise dating of core formation in iron meteorite parent bodies requires precise quantification of cosmic-ray effects on W isotopes but this has not been established yet.

* Corresponding author. Address: ETH Zurich, Institute of Isotope Geochemistry and Mineral Resources, Clausiusstr. 25, CH-8092 Zurich, Switzerland. Fax: +41 44 632 1827.
E-mail address: burkhardt@erdw.ethz.ch (C. Burkhardt).

0016-7037/$ - see front matter © 2008 Elsevier Ltd. All rights reserved.
doi:10.1016/j.gca.2008.10.023

1. INTRODUCTION

Key events in the early evolution of the solar system include the formation of Ca–Al-rich inclusions (CAIs) and chondrules as well as the accretion and subsequent differentiation of meteorite parent bodies. The sequence of these processes can be determined by applying short- and long-lived chronometers to meteorites and their components. For instance, absolute and relative ages of CAIs are the oldest yet obtained for any meteoritic material (Gray et al., 1973; Chen and Tilton, 1976; Lee et al., 1977; Chen and Wasserburg, 1981; Amelin et al., 2002), which is consistent with the mineralogy and chemical composition of CAIs that indicate formation from a gas of approximately solar composition (Grossman, 1972). Consequently, it has become customary to use the absolute age of CAIs as the age of the solar system. Chondrules are the major component of most chondrites and Al–Mg chronometry indicates that most chondrules formed ~2–3 Myr after CAIs (Russell et al., 1996; Kita et al., 2000; Huss et al., 2001; Hsu et al., 2003; Kunihiro et al., 2004; Rudraswami and Goswami, 2007; Kleine et al., 2008b; Kurahashi et al., 2008). In the classical model for the accretion and differentiation of asteroids, chondritic meteorites are considered to represent the material from which asteroids accreted and then differentiated. In this model, ages for CAIs and chondrules are interpreted to indicate that accretion of the first asteroids – as represented by chondritic meteorites – occurred ~2–3 Myr after condensation of CAIs, implying that the earliest point in time for differentiation of asteroids was ~2–3 Myr after CAI formation.

Application of ^{182}Hf–^{182}W chronometry to iron meteorites, however, has challenged this classical model for the accretion and differentiation of asteroids (Kleine et al., 2005; Markowski et al., 2006b; Schérsten et al., 2006; Qin et al., 2008b). Tungsten isotope data for CAIs and magmatic iron meteorites, generally considered to represent material from the metal cores of differentiated asteroids (Scott and Wasson, 1975), indicate that core formation in the parent bodies of magmatic iron meteorites predated chondrule formation (Kleine et al., 2005). Likewise, Al–Mg model ages for eucrites, angrites, and silicate inclusions from mesosiderites suggest that accretion of their parent bodies predated chondrule formation (Baker et al., 2005; Bizzarro et al., 2005) and ancient Pb–Pb and Mn–Cr ages for some eucrites (Lugmair and Shukolyukov, 1998; Nyquist et al., 2003; Amelin et al., 2006) provide evidence that magmatism on asteroids occurred contemporaneously with chondrule formation. These age constraints suggest that chondrule formation and hence accretion of chondrite parent bodies postdated the accretion of differentiated planetesimals.

The successful application of ^{182}Hf–^{182}W chronometry ($t_{1/2} = 8.90 \pm 0.09$ Ma) to early solar system processes requires precise knowledge of the Hf and W isotope compositions at the beginning of the solar system. This can be best obtained from CAIs because these are the oldest known objects formed within the solar system. Hence, the initial ^{182}W/^{184}W and ^{182}Hf/^{180}Hf of CAIs should provide a suitable starting point for constraining the duration of processes that took place in the early solar nebula. Owing to the limited number of samples and the rather narrow range in Hf/W ratios among the three CAIs for which Hf–W data are available (Yin et al., 2002; Kleine et al., 2005), the initial ^{182}Hf/^{180}Hf and ^{182}W/^{184}W ratios of the solar system are rather imprecisely defined and have uncertainties of ~10% and 0.2 ε (1ε = 0.01%), respectively. These are currently the major source of uncertainty in calculating Hf–W formation intervals relative to the formation of CAIs. For instance, in the first ~5 Myr after CAI formation the ^{182}W/^{184}W ratio of a reservoir with chondritic ^{180}Hf/^{184}W increases by ~0.1 ε/Myr, such that the initial ^{182}W/^{184}W of CAIs needs to be known precisely to resolve small time differences. Furthermore, some authors have argued that the Hf–W system in Allende CAIs has been reset during parent body processes and, hence, does not reflect the initial ^{182}Hf/^{180}Hf and ^{182}W/^{184}W ratios at the time of CAI formation (Humayun et al., 2007). Investigating the Hf–W systematics of CAIs, therefore, is important to better define the reference for calculating precise Hf–W ages and to verify whether core formation in some asteroids indeed predated chondrule formation.

The use of short-lived radionuclides as chronometers of the early solar system does not only require precise knowledge of their initial abundance in CAIs but also requires an assessment as to whether these values are representative of the entire solar system. This may not necessarily be the case, given that CAIs may have been exposed to an intensive irradiation near the early active Sun (Shu et al., 1997) and that some CAIs are enriched in *r*-process nuclides (Birck, 2004). An assessment of the homogeneity of short-lived nuclides in the early solar system can only be made if the initial abundances of short-lived nuclides are precisely known for CAIs and other early objects. Thus, precisely determining the initial ^{182}Hf/^{180}Hf of CAIs is essential for evaluating the distribution of short-lived nuclides in the early solar system.

We present Hf–W data for bulk samples and mineral separates from eight CAIs from the Allende and one CAI from the NWA 2364 carbonaceous chondrites. These data are used (i) to assess the possible presence of nucleosynthetic W isotope anomalies in CAIs, which may result from variable proportions of the products of *s*- and *r*-process nucleosynthesis, and (ii) to precisely define the initial ^{182}Hf/^{180}Hf and ^{182}W/^{184}W ratios at the time of CAI formation. These results are then used (i) to evaluate the consistency between the Hf–W and Al-Mg formation intervals between CAIs and angrites, (ii) to determine an absolute age of CAI formation, and (iii) to constrain the timescale of core formation in the parent bodies of magmatic iron meteorites.

2. SAMPLES AND ANALYTICAL METHODS

2.1. Sample description

All eight CAIs from the Allende CV3 chondrite are from the collection of the Naturmuseum Senckenberg in Frankfurt (Germany) and seven of these were separated from slices originally prepared at the Smithsonian Institution (Table 1). CAIs A-ZH-1 to -5 were used for bulk analyses.

Mineral separates were prepared from Allende CAIs A-ZH-6, -7, and -8 as well as from CAI N-ZH-9.

N-ZH-9 is a ~400 mg portion of a large (18 mm at greatest diameter) type B CAI from the NWA 2364 (CV3ox) chondrite containing coarsely crystalline melilite, fassaite, and anorthite (Friedrich et al., 2005). Fig. 1 shows an electron backscatter (BSE) image of a typical region near the rim of N-ZH-9. Interior fassaitic pyroxene (up to 19.1% TiO_2) regions reach up to 500 μm in diameter and are surrounded by melilite and/or anorthite. Melilite compositions tend from higher akermanite content in the central regions (Ak46 ± 15) to lower ones near the rim. Occasional secondary anorthite is present, especially near the rim. Spinel euhedra are heterogeneously distributed throughout each of the mineral phases discussed above.

Like N-ZH-9, most of the other investigated CAIs are also type B CAIs containing coarsely crystalline melilite and fassaite and minor anorthite. These include A-ZH-1, -3, and -4, and also A-ZH-7 and -8. A-ZH-2 is a ~175 mg portion of material from which the A44 type A CAI was separated (Floss et al., 1992). This remaining material contained abundant fassaite, which suggests that this CAI may be a type B inclusion, consistent with a recently suggested reclassification of A44 (Jacobsen et al., 2008). The classification of A-ZH-6 is less clear because it contains much less fassaite compared to the other type B inclusions investigated here and its light pink color is indicative of a relatively high modal abundance of spinel. A-ZH-5 is clearly different from all other CAIs investigated here. It shows a brittle texture, is finer grained and dominated by white- to variably pink-colored minerals, whereas fassaite is only minor or absent. A few relatively large (~100 μm) bluish grains (probably hibonite) were present. These observations together with the fluffy occurrence suggest that A-ZH-5 might be a fluffy type A CAI that experienced a high degree of secondary alteration.

CAIs A-ZH-7, -8, and N-ZH-9 contain metal, which was removed during sample preparation. The amount of metal that could be recovered, however, was insufficient to determine the W isotope composition of these metals. Several of the CAIs also contain sulphides, especially A-ZH-1 and -8.

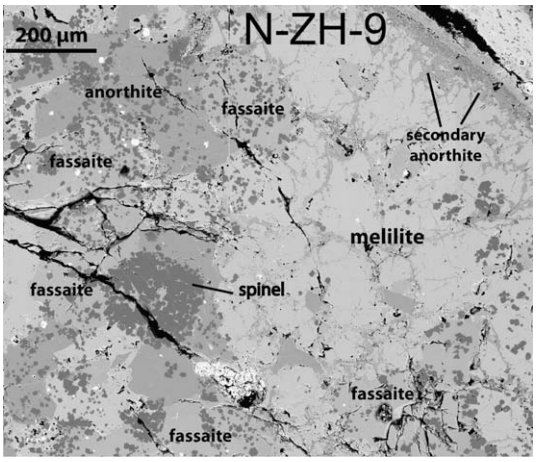

Fig. 1. Back-scattered electron image of a typical region of "The Crucible", a type B CAI from NWA 2364 (CV3ox), labeled as N-ZH-9 in this study. The majority of the coarsely crystalline fassaitic pyroxene (up to 19.1% TiO_2) regions (up to 500 μm in diameter) are typically surrounded by melilite (Ak46 ± 15) and primary anorthite. The relatively large fassaite and melilite grains were readily separable using the techniques described herein. Occasional secondary (alteration) anorthite is present near the rim, but is not extraordinarily abundant.

2.2. Analytical methods

Samples were cleaned with abrasive paper and by ultrasonication in 0.05 M HNO_3, distilled H_2O, and ethanol. They were carefully crushed in an agate mortar and CAI pieces were separated by handpicking under a binocular. Each piece was carefully inspected and only those pieces that did not contain any matrix material were selected. The remaining material, consisting of CAI and matrix material, was further crushed until the entire CAI was removed from the slice. Matrix dust adhering to the CAI pieces was removed by ultrasonication in distilled H_2O and ethanol. CAIs used for the bulk analyses were completely powdered in an agate mortar. CAIs used to obtain mineral separates were crushed and separated into <40 μm and 40 to 200 μm fractions using nylon sieves. Mineral separates were obtained from the 40 to 200 μm fractions by density separation using heavy liquids, additional handpicking and the use of a hand magnet. Three different fractions were prepared: a fassaite separate, a melilite-rich separate containing all minerals except fassaite and metal, and a mixed fraction. During preparation of these separates, all fassaites were removed from the melilite-rich fraction (as visible under a binocular), and metal was removed from the fassaite and melilite-rich fractions by repeated

Table 1
Characteristics of the CAIs analyzed in this study.

Sample	Host meteorite	Extracted material (mg)	Classification
A-ZH-1	Allende; USNM# 3529 slice C	~120	Type B
A-ZH-2	Allende; remaining part of A44	~180	Type A or B
A-ZH-3	Allende; USNM# 3515 slice Q	~70	Type B
A-ZH-4	Allende; USNM# 3529 slice C	~200	Type B
A-ZH-5	Allende; USNM# 3531 slice E	~90	Probably Type A
A-ZH-6	Allende; USNM# 3512 slice D	~200	Probably Type B
A-ZH-7	Allende; USNM# 3529 slice D	~350	Type B
A-ZH-8	Allende; USNM# 3531 slice E	~250	Type B
N-ZH-9	NWA 2364; the crucible	~400	Type B

grinding of the separates to fine powders and metal separation using a hand magnet.

Sample dissolution and separation of W from its sample matrix follows our previously established procedure (Kleine et al., 2004). Samples were dissolved in a 6:3:1 mixture of HF–HNO_3–$HClO_4$ on a hotplate at ~180 °C. After drying down, samples were redissolved and dried three times in HNO_3–H_2O_2 to destroy any organic matter. Samples were dissolved in ~15 ml 6 M HCl–0.06 M HF and total dissolution was achieved at this stage. Depending on the amount of W present, a 1–10% aliquot was spiked with a mixed ^{180}Hf–^{183}W tracer that was calibrated against pure Hf and W metals (Kleine et al., 2004). Spike-sample equilibration was achieved on a hotplate overnight.

After drying down, the aliquots for the W isotope composition measurements were redissolved in a 1 M HCl–0.5 M HF mixture and loaded onto pre-cleaned and conditioned anion exchange columns (3 ml Bio-Rad AG 1X8, 100–200 mesh). The matrix was rinsed off the columns using 5 ml of 0.5 M HCl–0.5 M HF and 3 ml 0.5 mM HCl–0.5 mM HF. Titanium was eluted with ~40 column volumes of 3.6 M HAc–8 mM HNO_3–2% H_2O_2 and Zr, Hf, and Nb were eluted with 9 ml 6 M HCl–0.01 M HF. Tungsten was then collected with 14 ml 6 M HCl–1 M HF. This chemical separation was repeated once to further purify the W-cut from the first chemistry. The main scope of the clean-up chemistry was to remove remaining Ti that was still present in the W-cut from the first step. The only difference from the first separation step is that the remaining traces of Zr, Nb, and Hf were eluted with 3 ml 6 M HCl–1 M HF instead of 9 ml 6 M HCl–0.01 M HF.

The spiked aliquots were dried, redissolved in 1.5 ml 1 M HCl–0.5 M HF and loaded onto precleaned and conditioned columns filled with 1 ml anion exchange resin (Bio-Rad AG 1X8, 200–400 mesh). After eluting the matrix with 5 ml of 1 M HF, Hf was eluted with 3 ml 6 M HCl–0.01 M HF followed by the elution of W with 4 ml 6 M HCl–1 M HF.

Total procedural blanks ranged from ~120 to ~820 pg for the W isotope composition measurements and were ~20 pg W and <8 pg Hf for the isotope dilution measurements. The variable W blanks are caused by the use of different amounts and different batches of acetic acid (Merck Suprapur®) that had variable W contents. Despite the occasionally high W blanks, blank corrections for the measurement of W isotopic compositions were always smaller than the analytical uncertainty. The largest blank correction of 0.36 ± 0.18 ε units was required for the fassaite separate of A-ZH-6.

All isotope measurements were performed on a *Nu Plasma* MC–ICP-MS at ETH Zurich. For measurements, the samples were re-dissolved and dried several times in HNO_3–H_2O_2 (and $HClO_4$ for some samples) to remove organic compounds and then taken up in 0.56 M HNO_3–0.24 M HF. Tungsten isotope compositions were typically measured with a signal intensity of ~3 V on ^{182}W, which was obtained for a ~30 ppb W solution. For these samples, 60 ratios (3 blocks of 20 ratios, 5 s integrations) were measured, resulting in within-run statistics on the order of 0.2 ε units (2σ). Owing to the small amount of W available from the fassaite-rich fraction of A-ZH-6, its W isotope composition was measured in 2 blocks of 20 ratios each with a signal intensities of ~1 V on ^{182}W. As described in detail in Kleine et al. (2008b), the external reproducibility of such W isotope measurements is similar to the within-run statistics. Small isobaric interferences of Os on masses 184 and 186 were corrected by monitoring ^{188}Os and were negligible. To assess possible matrix effects or artifacts due to improper mass bias correction, measured $^{182}W/^{183}W$, $^{182}W/^{184}W$ and $^{184}W/^{183}W$ ratios were normalized to $^{186}W/^{183}W$ and $^{186}W/^{184}W$ using the exponential law. We obtained the most reproducible results for normalization to $^{186}W/^{183}W$, which is therefore preferred. Unless stated otherwise, all W isotope data are reported relative to $^{186}W/^{183}W = 1.9859$. The $^{182}W/^{184}W$, $^{182}W/^{183}W$, and $^{184}W/^{183}W$ ratios of all samples were determined relative to two standard runs bracketing each sample run and are reported in $\varepsilon^{18i}W$ units, which is the deviation of the measured ratios from the terrestrial standard value in parts per 10,000. Repeated measurements of an Alfa Aesar standard metal during the course of this study yielded a mean $^{182}W/^{184}W = 0.864838 \pm 0.000038$ (2σ) and a mean $^{184}W/^{183}W = 2.14079 \pm 0.00007$ (2σ). The reproducibility of the ~30 ppb standard during one measurement day is typically equal to or better than ~0.3 ε units (2σ) for the $^{182}W/^{184}W$ ratio and ~0.2 ε units (2σ) for the $^{184}W/^{183}W$ ratio. The external reproducibility of the W isotope measurements was estimated from repeated measurements of several of the bulk rock CAIs (A-ZH-1, -2, and -5) and mineral separates (melilite-rich separate from A-ZH-7) and always is better than ~0.4 ε units (2SD) for both the $^{182}W/^{184}W$ and $^{184}W/^{183}W$ ratios. The accuracy of the measurements was monitored by analyzing some carbonaceous chondrites, all of which were consistent with the previously determined value of -1.9 ± 0.1 $\varepsilon^{182}W$ (Kleine et al., 2004).

For the Hf and W isotope dilution measurements, the uncertainties on the measured $^{180}Hf/^{177}Hf$ and $^{183}W/^{184}W$ ratios were better than 0.2% (2σ) in most cases. The main source of error in the determination of Hf/W ratios is the correction for the W blank with sample/blank ratios between 45 and 200 for most samples. Assuming a 50% uncertainty for the correction of W blank – which probably is overestimating the uncertainty given that the main source of the blank are the acids – the resulting uncertainty in the Hf/W ratios are better than ± 1% (2σ) in most and better than ± 2% (2σ) in all cases.

3. RESULTS

The Hf–W data for five bulk CAIs from Allende are reported in Table 2 and shown in Fig. 2. The Hf and W contents of the five bulk CAIs investigated here are relatively constant and range from ~1.6 to ~2.1 ppm Hf and ~1 to ~1.3 ppm W. Although we did not obtain "whole-rock" Hf–W data for those CAIs that were used to determine internal Hf–W isochrons, the combined Hf and W contents of the separated phases of these CAIs are consistent with the range given by the Hf–W data for the bulk CAIs. The only exception is A-ZH-6, which has much lower Hf and W contents (Table 3). Allende bulk CAIs A-ZH-1 to -4 ex-

Table 2
Hf–W data for bulk CAIs.[a]

Sample	Hf (ppm)	W (ppm)	$^{180}Hf/^{184}W \pm 2\sigma$	$\varepsilon^{182}W/^{183}W$ (6/3) $\pm 2\sigma$	$\varepsilon^{182}W/^{184}W$ (6/4) $\pm 2\sigma$	$\varepsilon^{182}W/^{184}W$ (6/3) $\pm 2\sigma$	$\varepsilon^{184}W/^{183}W$ (6/3) $\pm 2\sigma$
A-ZH-1	1.595	1.026	1.83 ± 1	-1.15 ± 0.19	-1.08 ± 0.21	-1.14 ± 0.17	0.01 ± 0.12
				-1.87 ± 0.49	-1.15 ± 0.45	-1.51 ± 0.38	-0.41 ± 0.27
				-1.65 ± 0.23	-1.54 ± 0.25	-1.56 ± 0.20	-0.05 ± 0.13
				-1.32 ± 0.15	-1.16 ± 0.18	-1.30 ± 0.12	-0.02 ± 0.11
Mean				-1.50 ± 0.52	-1.23 ± 0.34	-1.38 ± 0.31	-0.12 ± 0.31
A-ZH-2	2.087	1.218	2.02 ± 1	-1.34 ± 0.20	-0.89 ± 0.21	-1.02 ± 0.14	-0.26 ± 0.15
				-1.33 ± 0.15	-0.83 ± 0.18	-1.04 ± 0.12	-0.26 ± 0.11
				-1.15 ± 0.12	-0.79 ± 0.16	-0.97 ± 0.12	-0.20 ± 0.09
				-1.10 ± 0.18	-0.78 ± 0.20	-0.93 ± 0.16	-0.15 ± 0.11
				-1.05 ± 0.20	-0.61 ± 0.19	-0.89 ± 0.16	-0.21 ± 0.12
				-1.25 ± 0.17	-0.92 ± 0.16	-1.07 ± 0.14	-0.07 ± 0.11
Mean				-1.20 ± 0.13	-0.80 ± 0.12	-0.99 ± 0.07	-0.19 ± 0.08
A-ZH-3	1.565	1.158	1.60 ± 1	-6.36 ± 0.15	-1.39 ± 0.14	-3.92 ± 0.12	-2.48 ± 0.08
				-6.28 ± 0.24	-1.43 ± 0.23	-3.90 ± 0.18	-2.37 ± 0.15
Mean				-6.32 ± 0.45	-1.41 ± 0.45	-3.91 ± 0.40	-2.43 ± 0.40
A-ZH-4	1.731	0.9625	2.12 ± 1	-1.15 ± 0.24	-0.33 ± 0.19	-0.85 ± 0.16	-0.44 ± 0.15
				-1.36 ± 0.17	-0.77 ± 0.19	-1.10 ± 0.12	-0.28 ± 0.12
Mean				-1.25 ± 0.45	-0.55 ± 0.45	-0.98 ± 0.40	-0.36 ± 0.40
A-ZH-5	2.046	1.352	1.79 ± 1	-1.14 ± 0.18	2.29 ± 0.20	0.59 ± 0.15	-1.73 ± 0.11
				-1.33 ± 0.18	2.26 ± 0.17	0.47 ± 0.14	-1.82 ± 0.10
				-0.95 ± 0.25	2.10 ± 0.23	0.57 ± 0.19	-1.59 ± 0.14
Mean				-1.14 ± 0.47	2.21 ± 0.25	0.54 ± 0.16	-1.71 ± 0.30

[a] For the $^{180}Hf/^{184}W$ ratios ($^{180}Hf/^{184}W = 1.18 \times Hf/W$) uncertainties refer to the last significant digits. For samples that were measured more than once, the 2σ uncertainties for each individual run are given. For samples that were measured more than two times, the 2σ uncertainties for the mean W isotope ratios were calculated using $\sigma \times t_{0.95,n-1}/\sqrt{n}$. For samples that were measured only once or twice, the standard deviation (2σ) estimated from repeated analyses for several samples is given. (6/3) and (6/4) denote mass bias correction relative to $^{186}W/^{183}W$ and $^{186}W/^{184}W$, respectively.

hibit a narrow range in $^{180}Hf/^{184}W$ ratios (1.6–2.1; where $^{180}Hf/^{184}W = 1.18 \times Hf/W$) and $\varepsilon^{182}W$ values (-1.4 to -1.0). Both Hf/W ratios and $\varepsilon^{182}W$ values are slightly elevated relative to average carbonaceous chondrites [$^{180}Hf/^{184}W = 1.25$, $\varepsilon^{182}W = -1.9$; Kleine et al. (2004)]. The $^{180}Hf/^{184}W$ ratio of A-ZH-5 is 1.8 and hence well within the range obtained for the other bulk CAIs investigated here but its W isotopic composition appears to be anomalous. The $^{182}W/^{184}W$ ratio (normalized to $^{186}W/^{183}W$ or $^{186}W/^{184}W$) yields much higher $\varepsilon^{182}W$ than those of the other bulk CAIs but using the $^{182}W/^{183}W$ ratio (normalized to $^{186}W/^{183}W$) gives $\varepsilon^{182}W \sim -1.14$, within the range of $\varepsilon^{182}W$ values obtained for the other bulk CAIs. The $^{184}W/^{183}W$ ratios for most of the bulk CAIs and mineral separates are identical to the terrestrial standard value and only for few samples $^{184}W/^{183}W$ ratios ~1–2.5 ε units lower than the standard value were observed.

The Hf–W data for mineral separates of the Allende CAIs A-ZH-6, A-ZH-7, A-ZH-8 and the NWA2364 CAI N-ZH-9 are given in Table 3 and shown in Figs. 3 and 4. Except for A-ZH-8, the W contents among the different separates of the CAIs are relatively constant but Hf contents are variable. Fassaites always have the highest Hf contents, and the melilite-rich separates the lowest, which is consistent with trace element data for CAI minerals reported earlier (Simon et al., 1991; Palme et al., 1994). Accordingly, fassaites have the highest $^{180}Hf/^{184}W$ and $\varepsilon^{182}W$, whereas the melilite-rich separates have the lowest $^{180}Hf/^{184}W$ and $\varepsilon^{182}W$. The same pattern is observed for mineral separates from A-ZH-8 except that they exhibit a much larger range in W contents than is observed for the other CAIs. For all CAIs, the $\varepsilon^{182}W$ values for the mineral separates correlate with their Hf/W ratios and all the separates with the exception of two fractions from A-ZH-8 plot on a single isochron. The bulk CAIs investigated here and the previously investigated CAIs A37, A44a, and All-MS-1 as well as average carbonaceous chondrites also plot on this isochron (Fig. 4).

4. NUCLEOSYNTHETIC W ISOTOPE ANOMALIES IN CAIS

Nucleosynthetic isotope anomalies for various elements were reported in some CAIs and many CAIs from CV3 chondrites show *r*-process enrichments (Birck, 2004). The presence of excesses or depletions in *s*- and *r*-process components may affect the W isotope composition of CAIs and must be assessed before W isotope data for CAIs can be

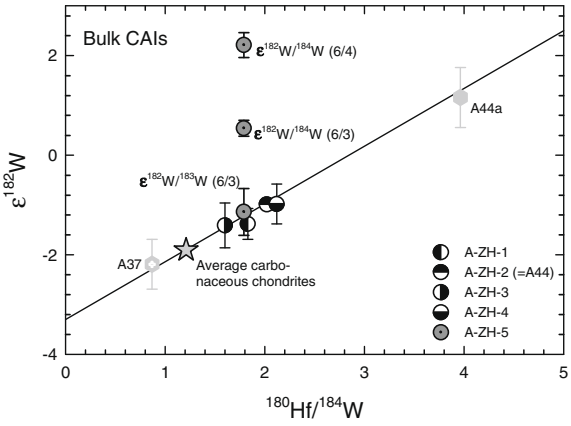

Fig. 2. Hf–W isochron for bulk CAIs obtained in this study. Hf–W data for average carbonaceous chondrites (Kleine et al., 2004) and CAIs A37 (Kleine et al., 2005) and A44a (Yin et al., 2002) are also shown. For most samples the $^{182}W/^{184}W$ ratios normalized to $^{186}W/^{183}W$ are shown, except for A-ZH-3, which has a measured $^{184}W/^{183}W$ that is lower than the terrestrial standard value. This is most likely caused by a small isobaric interference on mass 183 and the $^{182}W/^{184}W$ ratio normalized to $^{186}W/^{184}W$ is used instead. For A-ZH-5, $\varepsilon^{182}W$ values calculated using three different normalization procedures are shown. This CAI has a ^{184}W deficit, most likely caused by an overabundance of *r*-process isotopes in this CAI (see Fig. 5). Note that the $\varepsilon^{182}W/^{183}W$ (normalized to $^{186}W/^{183}W$) of this CAI is identical to $\varepsilon^{182}W$ values for the other CAIs. The solid line is the combined CAI isochron shown in Fig. 4. The CAIs investigated here show a narrow range in $^{180}Hf/^{184}W$ and $\varepsilon^{182}W$, which precludes determination of a CAI whole-rock isochron. Note that the Hf–W data for A37 and A44a are not representative for the bulk composition of these CAIs.

interpreted in terms of chronology. Quantifying the effects that a heterogeneous distribution of these two components would have on the W isotope composition requires knowledge of the *s*- and *r*-process yields for each of the W isotopes. These have recently been estimated by Qin et al. (2008a) and these authors show that the *s*-process produces significantly more ^{184}W than the *r*-process and that different proportions of *s*- and *r*-process components should result in a correlation between $\varepsilon^{184}W$ and $\varepsilon^{182}W$ anomalies (normalized to a given $^{186}W/^{183}W$) (Qin et al., 2008a). The slope of this correlation line depends on the calculated *s*-process composition of W isotopes, which in turn depend on the neutron-capture cross sections of the stable W isotopes and the cross sections and β^-–decay rates at the relevant branching points. Using recommended values of Maxwellian-averaged cross sections (MACS), Qin et al. (2008a) obtained a slope for the $\varepsilon^{182}W$–$\varepsilon^{184}W$ correlation line of $\sim 0.04 \pm 0.20$ (i.e., ^{184}W anomalies should be $\sim$25 times larger than ^{182}W anomalies). However, these authors also note that the cross section of ^{182}W might be $\sim$20% lower, in which case the slope of the $\varepsilon^{182}W$–$\varepsilon^{184}W$ correlation line would be $\sim$0.5.

In Fig. 5, which is adopted from Qin et al. (2008a), the expected $\varepsilon^{182}W$ and $\varepsilon^{184}W$ variations that are due to the presence of different proportions of *s*- and *r*-process W isotopes are shown together with W isotope data for the five bulk CAIs investigated here. Fig. 5 illustrates that three of the five bulk CAIs (A-ZH-1, -2, and -4) studied here have $^{184}W/^{183}W$ ratios identical within analytical uncertainty to those of the terrestrial standard. The $^{184}W/^{183}W$ ratio of A-ZH-2 is only marginally lower than the value of the terrestrial standard but this small anomaly of $\sim$20 ppm is currently not well resolved. The $^{184}W/^{183}W$ of these three CAIs is also indistinguishable from values obtained for bulk carbonaceous and ordinary chondrites as well as other groups of meteorites (iron meteorites and eucrites), indicating that these CAIs have a W isotope composition indistinguishable from that of the average solar system.

CAI A-ZH-5 exhibits a $\sim$1.7-ε unit deficit in ^{184}W, whereas its $^{182}W/^{183}W$ ratio (normalized to $^{186}W/^{183}W$) is indistinguishable from those of the other CAIs (with the exception of A-ZH-3, see below). This is consistent with predictions from the standard MACS model shown in Fig. 5 and suggests that A-ZH-5 is enriched in *r*-process relative to *s*-process isotopes. In contrast, the measured $\varepsilon^{182}W$ and $\varepsilon^{184}W$ values of A-ZH-3 cannot be of nucleosynthetic heritage because this sample plots far outside the field of possible nucleosynthetic W isotope anomalies (Fig. 5).

The anomalous measured W isotope composition of A-ZH-3 is most likely caused by an occasionally occurring interference on mass 183, which probably is due to the presence of organics (Fig. 5). Such interferences were observed previously in several other W isotope studies. For example, elevated $^{183}W/^{184}W$ ratios were reported for some eucrites (Kleine et al., 2004) and these were clearly attributable to interferences on mass 183 because the $^{182}W/^{184}W$ ratios (when mass bias corrected using $^{186}W/^{184}W$) of these eucrites are consistent with the Hf–W data for other eucrites (Kleine et al., 2004). Similar observations were made for some non-magnetic fractions of a few H chondrites (Kleine et al., 2008b). In most cases, this organic interference can be removed by repeated treatment of the sample with HNO_3–H_2O_2. The two CAIs that show anomalous $^{184}W/^{183}W$ were therefore treated several times with HNO_3–H_2O_2 and also $HClO_4$ but for both CAIs this procedure could not reduce the $^{184}W/^{183}W$ anomaly. This and the W isotope data for some of the separates from A-ZH-6 and -8 indicates that our procedure has not always entirely removed the interference on mass 183 because some of these separates show lower $^{184}W/^{183}W$ whereas others from the same CAIs do not (Table 2). It is highly unlikely that individual minerals from one of these CAIs have distinct abundances of ^{183}W, ^{184}W, or ^{186}W, given that these CAIs formed by crystallization from a melt. Therefore, the negative $\varepsilon^{184}W$ values of some A-ZH-6 and -8 separates and bulk CAI A-ZH-3 are most likely caused by an interference on mass 183. Note that their $^{182}W/^{184}W$ ratios (normalized to $^{186}W/^{184}W$) are consistent with the Hf–W data for the other CAIs.

5. HF–W CHRONOMETRY OF CAIS

5.1. Internal Hf–W isochrons of CAIs: improved initial Hf and W isotope compositions

To define an internal Hf–W isochron, the minerals of a CAI must meet the following conditions: (i) they must have had the same initial W isotopic composition, i.e., they must

Table 3
Hf–W data for mineral separates from CAIs.[a]

Sample	Hf (ppm)	W (ppm)	$^{180}Hf/^{184}W \pm 2\sigma$	$\varepsilon^{182}W/^{183}W$ (6/3) $\pm 2\sigma$	$\varepsilon^{182}W/^{184}W$ (6/4) $\pm 2\sigma$	$\varepsilon^{182}W/^{184}W$ (6/3) $\pm 2\sigma$	$\varepsilon^{184}W/^{183}W$ (6/3) $\pm 2\sigma$
A-ZH-6							
Melilite-rich	0.3841	0.4250	1.07 ± 1	−2.10 ± 0.45	−1.92 ± 0.45	−2.00 ± 0.40	−0.11 ± 0.40
Mixed	1.670	0.4602	4.28 ± 4	−0.23 ± 0.45	1.66 ± 0.45	0.58 ± 0.40	−1.06 ± 0.40
Fassaite[b]	3.72	0.343	12.8 ± 2	11.7 ± 1.0	11.8 ± 1.2	11.7 ± 1.0	−0.20 ± 0.40
A-ZH-7							
Melilite-rich	0.7964	1.140	0.82 ± 1	−2.64 ± 0.18	−2.75 ± 0.19	−2.68 ± 0.15	0.01 ± 0.10
				−2.34 ± 0.16	−2.55 ± 0.17	−2.37 ± 0.14	0.12 ± 0.12
				−2.32 ± 0.20	−2.27 ± 0.21	−2.27 ± 0.17	0.03 ± 0.10
				−2.16 ± 0.16	−2.20 ± 0.21	−2.14 ± 0.15	0.10 ± 0.10
				−2.32 ± 0.20	−2.45 ± 0.22	−2.47 ± 0.17	0.07 ± 0.13
Mean				−2.35 ± 0.22	−2.45 ± 0.28	−2.39 ± 0.26	0.06 ± 0.06
Mixed	2.588	1.300	2.35 ± 2	−0.76 ± 0.17	−0.65 ± 0.19	−0.71 ± 0.15	−0.10 ± 0.11
				−0.39 ± 0.30	−0.54 ± 0.46	−0.56 ± 0.33	−0.08 ± 0.24
Mean				−0.58 ± 0.45	−0.59 ± 0.45	−0.64 ± 0.40	−0.01 ± 0.40
Fassaite	5.281	1.149	5.42 ± 6	2.33 ± 0.45	2.71 ± 0.45	2.48 ± 0.40	−0.20±0.40
Fines	2.021	1.154	2.07 ± 2	−1.23 ± 0.45	−0.66 ± 0.45	−0.99 ± 0.40	−0.26 ± 0.40
A-ZH-8							
Melilite-rich	0.5244	0.5923	1.04 ± 1	−2.08 ± 0.17	−2.12 ± 0.21	−2.07 ± 0.16	−0.03 ± 0.09
				−1.93 ± 0.22	−2.01 ± 0.22	−1.90 ± 0.16	0.08 ± 0.13
Mean				−2.00 ± 0.45	−2.06 ± 0.45	−1.98 ± 0.40	0.02 ± 0.40
Mixed	2.467	1.151	2.53 ± 2	−0.48 ± 0.45	−0.58 ± 0.45	−0.55 ± 0.40	0.04 ± 0.40
Fassaite[b]	6.754	1.730	4.61 ± 2	−0.04 ± 0.45	3.00 ± 0.91	1.35 ± 0.50	−1.42 ± 0.40
Fines	1.416	1.197	1.40 ± 1	−2.94 ± 0.45	−0.88 ± 0.45	−1.88 ± 0.40	−1.05 ± 0.40
N-ZH-9							
Melilite-rich	0.7947	1.174	0.799 ± 4	−2.12 ± 0.45	−2.60 ± 0.45	−2.41 ± 0.40	0.18 ± 0.40
Mixed	2.421	1.461	1.96 ± 1	−1.17 ± 0.45	−1.15 ± 0.45	−1.11 ± 0.40	0.07 ± 0.40
Fassaite	4.380	0.9081	5.69 ± 4	3.31 ± 0.45	2.95 ± 0.45	3.07 ± 0.40	0.14 ± 0.40
Fines	1.705	1.319	1.526 ± 6	−1.34 ± 0.20	−1.35 ± 0.23	−1.28 ± 0.19	0.05 ± 0.15
				−1.20 ± 0.21	−1.65 ± 0.20	−1.41 ± 0.14	0.27 ± 0.13
Mean				−1.27 ± 0.45	−1.50 ± 0.45	−1.34 ± 0.40	0.16 ± 0.40

[a] For the $^{180}Hf/^{184}W$ ratios ($^{180}Hf/^{184}W = 1.18 \times Hf/W$) uncertainties refer to the last significant digits. For samples that were measured more than once, the 2σ uncertainties for each individual run are given. For samples that were measured more than two times, the 2σ uncertainties for the mean W isotope ratios were calculated using $\sigma \times t_{0.95,n-1}/\sqrt{n}$. For samples that were measured only once or twice, the standard deviation (2σ) estimated from repeated analyses for several samples is given. (6/3) and (6/4) denote mass bias correction relative to $^{186}W/^{183}W$ and $^{186}W/^{184}W$, respectively.

[b] Blank corrected values; before correction the $\varepsilon^{182}W/^{184}W$ values were 11.46 ± 0.81 (6/4), 11.35 ± 0.62 (6/3) and 2.77 ± 0.65 (6/4) for the fassaite-rich separates from A-ZH-6 and -8, respectively.

initially have been in isotopic equilibrium; (ii) they must have remained as a closed system with respect to Hf and W. If these conditions are met, then the lines in the $\varepsilon^{182}W$ versus $^{180}Hf/^{184}W$ diagrams for CAIs define the initial $\varepsilon^{182}W$ and $^{182}Hf/^{180}Hf$ at the time of the last isotope equilibration. The first of these assumptions is likely to be valid because type B CAIs formed by crystallization from a melt (MacPherson, 2007), such that potential initial W isotopic heterogeneities among different phases probably were homogenized. The second assumption, closed-system behavior for Hf and W, is more difficult to assess but we will show below that for most of the investigated CAIs this condition is valid.

Numerous studies have reported disturbed isotopic systematics in Allende CAIs that probably reflect late open-system behavior caused by parent body processes (Gray et al., 1973; Chen and Tilton, 1976; Tatsumoto et al., 1976; Chen and Wasserburg, 1981; Podosek et al., 1991; Becker et al., 2001). Moreover, although the major and trace element composition of CAIs is broadly consistent with formation from a gas of solar composition (Grossman, 1972), most show evidence for complex histories and some CAIs were extensively altered (Grossman, 1980; MacPherson et al., 1988; MacPherson, 2007).

The evidence for disturbed isotope systematics in many Allende CAIs raises the question as to whether the Hf–W system in the CAIs investigated here has been disturbed. Parent body processes can affect the isotope systematics in two different ways. First, low-temperature alteration can result in the redistribution of Hf and W, rendering it possible that the $\varepsilon^{182}W$-$^{180}Hf/^{184}W$ correlation lines are not isochrons but mixing lines. Second, thermal metamorphism can facilitate isotopic exchange within CAIs, as for instance has been observed for the Al–Mg systematics of melilite and anorthite in some Allende CAIs (Podosek et al., 1991).

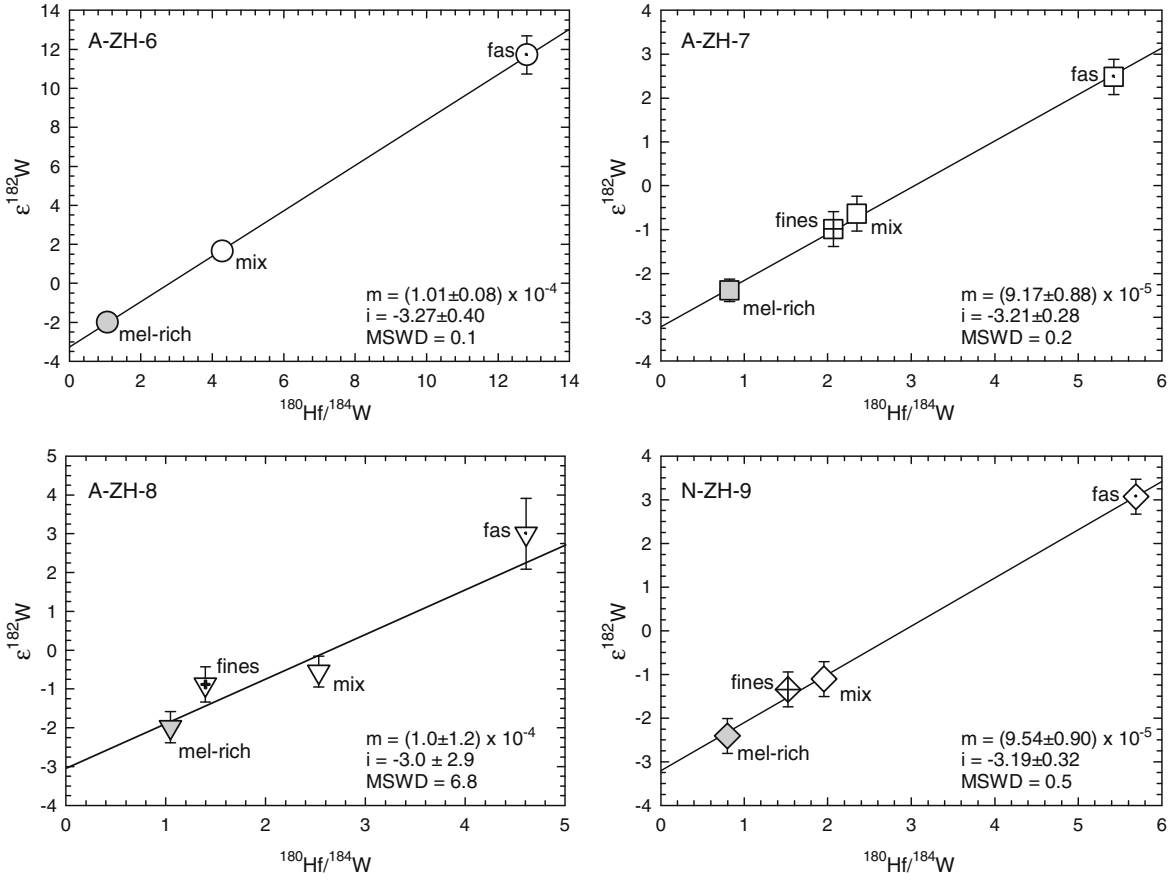

Fig. 3. Internal Hf–W isochrons for CAIs. m, initial $^{182}Hf/^{180}Hf$; i, initial $\varepsilon^{182}W$; fas, fassaite; mel, melilite. Regressions were calculated using the model 1 fit of ISOPLOT (Ludwig, 1991) and using uncertainties as reported in Tables 2 and 3. For most samples, the $^{182}W/^{184}W$ ratios normalized to $^{186}W/^{183}W$ are shown, except for three fractions (one from A-ZH-6, two from A-ZH-8) with negative measured $\varepsilon^{184}W$. These are attributed to small isobaric interferences on mass 183 and the $^{182}W/^{184}W$ ratio normalized to $^{186}W/^{184}W$ is used instead.

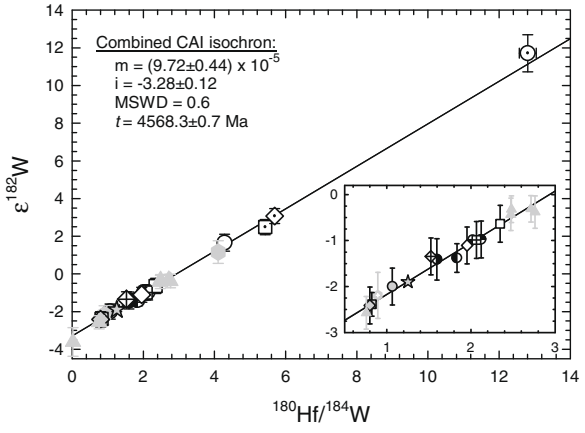

Fig. 4. Combined Hf–W isochron for CAIs. Symbols and regression as in Figs. 2 and 3. Grey triangles are data for different fractions from Allende CAI All-MS-1 (Kleine et al., 2005). Inset shows a magnification of the isochron with Hf–W data for fractions with low $^{180}Hf/^{184}W$. The absolute age is calculated relative to Pb–Pb ages for angrites (for details see text).

5.1.1. Hosts of Hf and W in CAIs

Interpreting the Hf–W data for mineral separates from CAIs requires some knowledge about the host minerals of Hf and W in CAIs. Type B CAIs consist predominantly of fassaite, melilite, anorthite, and spinel (Grossman, 1980). Important accessory phases include metal and perovskite. The former occur as inclusions within primary CAI phases: 70–80% are found in fassaites and the remaining 20–30% occur in spinel, melilite and anorthite (El Goresy et al., 1978). Perovskite is rare in type B CAIs but several occurrences have been documented, especially in CAIs from CV chondrites (e.g., Fuchs, 1978; Kornacki and Wood, 1985).

For anorthite, spinel, and melilite, mineral–melt partition coefficients for Hf (D_{Hf}) are $\sim 10^{-3}$ (Simon et al., 1994; Lundstrom et al., 2006), such that these minerals cannot be important hosts for Hf. In contrast, fassaite has $D_{Hf} \sim 1.5$–2 (Simon et al., 1991) and, due to its high modal abundance, is the major host of Hf in type B CAIs. Another important Hf host is perovskite, which in CAIs is stochiometric $CaTiO_3$. Reported D_{Hf} values for perovskite range from ~0.1 to 5 (Kennedy et al., 1993; Corgne and Wood, 2002) and this range in values probably reflects differences in experimental conditions. Nevertheless, these values show that perovskite can contain appreciable amounts of Hf, possibly even more than fassaites. No Hf concentration data have been reported for perovskite in CAIs but Simon et al. (1994) determined enrichment factors relative to CI

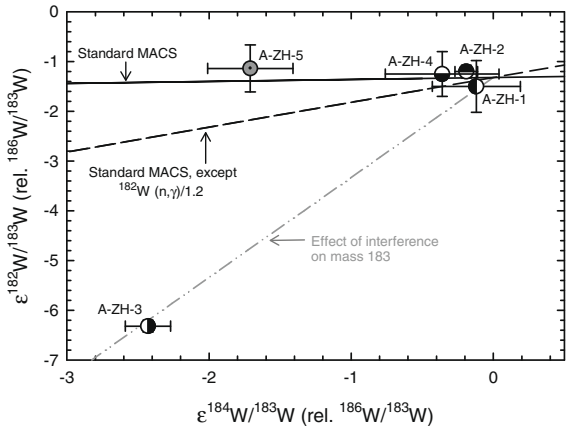

Fig. 5. Correlation between $\varepsilon^{184}W$ and $\varepsilon^{182}W$ (both normalized to $^{186}W/^{183}W$) for various proportions of *s*- and *r*-process W in CAIs, adopted from Fig. 7 of Qin et al. (2008a). The $\varepsilon^{184}W$–$\varepsilon^{182}W$ correlation lines were calculated by Qin et al. (2008a) using recommended values of Maxwellian-averaged (n,γ) cross sections (MACS). The dashed line is obtained by using a ~20% reduction in the ^{182}W cross section, which would be required to yield more realistic results for the ^{182}W *r*-process component (see Qin et al., 2008a). The grey dashed-dotted line shows the effect that an interference on mass 183 has on the measured $\varepsilon^{182}W$ and $\varepsilon^{184}W$ values. The measured W isotope composition of A-ZH-3 is consistent with such an interference.

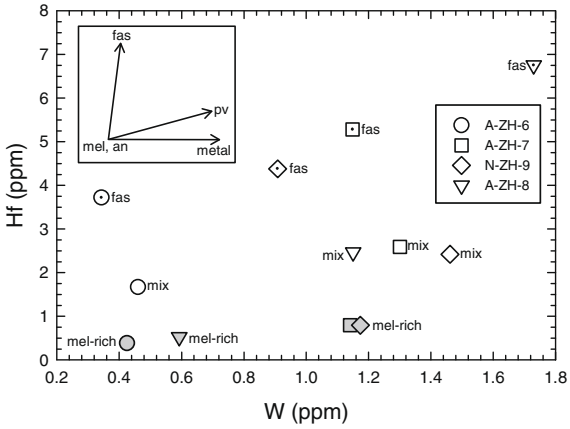

Fig. 6. Hf and W concentrations in different CAI separates. The data require the presence of at least three independent components for Hf and W among the coexisting phases in CAIs.

chondrites of 30–1000 for Zr in perovskites from compact type A CAIs. If, as seems likely, Hf is similarly enriched, then the Hf concentration in perovskite could be as high as ~100 ppm.

The major hosts of W (and other refractory siderophile elements) in CAIs are μm-size metal alloys and larger aggregates of metal, oxide, sulphide and silicate phases (Palme and Wlotzka, 1976; El Goresy et al., 1978; Bischoff and Palme, 1987; Blum et al., 1989; Sylvester et al., 1990; Palme et al., 1994). The refractory metal nuggets were initially termed Fremdlinge (El Goresy et al., 1978) but later it was proposed that the term 'opaque assemblages' is more appropriate (Blum et al., 1989). Their formation has been attributed to condensation from a nebular gas (Armstrong et al., 1987; Bischoff and Palme, 1987; Palme et al., 1994) or to exsolution, sulfidation, and oxidation of precursor alloys during low-temperature alteration on the parent body (Blum et al., 1989).

The W contents in other CAI minerals are more difficult to estimate because there are no experimentally determined D_W values available for any of the aforementioned minerals. The low D_W values in high-Ca pyroxene and plagioclase (Righter and Shearer, 2003) as well as low W concentrations in fassaites from Efremovka and Allende CAIs (Humayun et al., 2007) suggest that fassaites and anorthite have low W contents. For spinel and melilite the situation is less clear but given that elements such as Hf, Ta, U, and Th, which have ionic radii and charges that are similar to those of W, do not partition into spinel and melilite (Lundstrom et al., 2006) it seems unlikely that these minerals contain significant amounts of W. This is consistent with low W contents in spinel and melilite from Efremovka CAI Ef2 (Humayun et al., 2007). There are no experimental data for partitioning of W into $CaTiO_3$ but the D_W value may be estimated from the lattice strain model for $CaTiO_3$ presented by Corgne and Wood (2002). If W has a charge of +4 and occurs in 6-fold coordination, then its ionic radius is 0.066 nm (Shannon, 1976) and D_W is ~0.5. Note that in the same model D_{Hf} is ~0.1 such that perovskite might be characterized by a relatively low Hf/W ratio. Although the exact value of D_W remains poorly constrained – because W may occur in a different coordination – this estimate reveals that perovskite may contain appreciable amounts of W.

Fig. 6 reveals that the Hf and W concentrations of the mineral separates from the CAIs investigated here are not collinear for any of the CAIs in a binary Hf–W diagram, indicating the presence of at least *three* independent components for Hf and W among the coexisting phases. This is consistent with the mineral-melt partition coefficients summarized above. The three components are (i) fassaite with high Hf contents, (ii) the opaque assemblages, which are virtually Hf-free but enriched in W, and (iii) the melilite-rich fraction, which is characterized by relatively low Hf and W contents. The Hf contents of the melilite-rich fractions are too high to be accommodated by melilite, anorthite or spinel. Thus, the melilite-rich fractions must contain a Hf-bearing mineral but this cannot be fassaite because the melilite-rich separates would need to contain ~10% fassaites (with 3.7–6.8 ppm Hf, see Table 3) to account for their observed Hf content (~0.4–0.8 ppb). Based on the optical inspection of the separates under a binocular microscope this can be excluded. Thus, the host of Hf in the melilite-rich separates must be a different mineral and the only viable candidate is perovskite, which may contain up to ~100 ppm Hf (see above).

From the lattice strain model of $CaTiO_3$ it is expected that perovskite has a low Hf/W ratio but no W concentration data for perovskite have been obtained yet. However, the Hf–W data for different CAI fractions obtained for the present study suggest perovskite contains appreciable amounts of W. Given that fassaites contain the majority

of opaque assemblages, the lower or equal W contents of fassaites compared to the melilite-rich separates from CAIs A-ZH-6 and -7 and N-ZH-9 suggests that our procedure has largely removed the metal inclusions from these separates (Fig. 6). Therefore, the different W contents of the fassaite and melilite-rich separates probably do not reflect variable metal contents in these separates but are due to the presence of perovskite in these separates. It is important to note that in CAIs perovskite occurs mainly associated with melilite and spinel (e.g., Grossman, 1975; Bischoff and Palme, 1987) and this could account for the higher W content of the melilite-rich separates compared to the fassaites.

5.1.2. Internal isochrons vs. mixing lines

Given the evidence for late open-system behavior of highly siderophile elements on the chondrite parent bodies (Becker et al., 2001; Walker et al., 2002; Horan et al., 2003), it seems likely that to some extent W was also mobilized and redistributed. For instance, high W contents in a sulphide vein from Allende CAI TS68 (Campbell et al., 2003) and the occurrence of secondary W-rich phases such as scheelite in some CAIs (Armstrong et al., 1987; Bischoff and Palme, 1987; Blum et al., 1989) may reflect such redistribution processes. This raises the question as to whether the correlation of $\varepsilon^{182}W$ with $^{180}Hf/^{184}W$ obtained for mineral separates from individual CAIs are not isochrons but mixing lines between primary fassaites and opaque assemblages. Such a mixing line might not have chronological significance and might provide initial $^{182}W/^{184}W$ and $^{182}Hf/^{180}Hf$ ratios that are higher and lower, respectively, than the values at the time of CAI formation (see mixing line between metal B and fassaite in Fig. 8). There are two scenarios by which opaque assemblages could have acquired a $^{182}W/^{184}W$ ratio that is higher than the value at the time of the last isotope equilibration inside CAIs: (i) during parent body alteration W from the Allende matrix was transported into CAIs and was mixed with W from the opaque assemblages. Since W from the Allende matrix might have had an elevated $^{182}W/^{184}W$ ratio, such a process could have resulted in an increase in the $^{182}W/^{184}W$ of the opaque assemblages; (ii) during CAI alteration radiogenic W from some fassaites inside the CAIs was released and added to the opaque assemblages. Note that this process is different from isotopic exchange between fassaites and opaque assemblages because the W isotope composition of primary fassaites would have remained unchanged. Whether isotopic exchange between fassaites and opaque assemblages (which requires heating above the closure temperature of the Hf–W system in CAIs) could have occurred during parent body metamorphism will be discussed in Section 5.1.3 below.

Several lines of evidence indicate that the correlation of $\varepsilon^{182}W$ with $^{180}Hf/^{184}W$ obtained for mineral separates from CAIs is not a mixing line between opaque assemblages and primary fassaite.

In a plot of $\varepsilon^{182}W$ vs. 1/W, binary mixtures of a W-rich (opaque assemblages) and a W-poor (primary fassaite) endmember should define a straight line. This is not observed for the CAIs investigated here (Fig. 7) and the lack of a correlation in the $\varepsilon^{182}W$ vs. 1/W plot provides unequivocal evidence that the $\varepsilon^{182}W$-$^{180}Hf/^{184}W$ correlation observed for CAIs cannot be a mixing line.

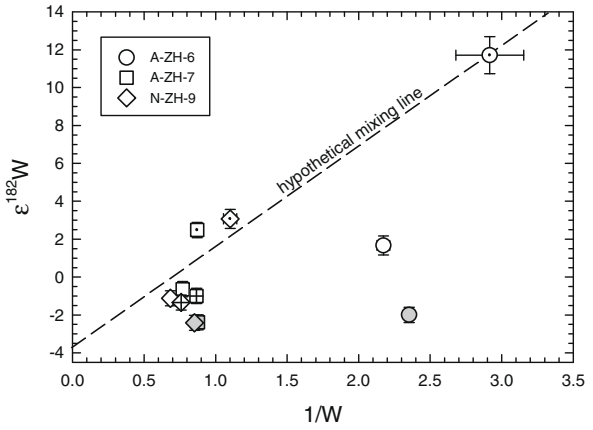

Fig. 7. $\varepsilon^{182}W$ vs. 1/W diagram, in which binary mixtures form straight lines. A hypothetical mixing curve between the most radiogenic fassaites and metal having $\varepsilon^{182}W \sim -3.7$ is shown. The mineral separates analyzed for the present study do not plot on straight lines, indicating that the Hf–W systematics do not reflect simple binary mixing. Symbols are as in Fig. 3.

Humayun et al. (2007) stated that in CAIs metal is the *sole* host of W and fassaite is the *sole* host of Hf. However, the Hf–W data for the mineral separates from the CAIs investigated here require the presence of at least *three* independent components for Hf and W: fassaite, metal, and perovskite (see above). Thus, the Hf–W systematics cannot be interpreted in terms of a two-component mixture.

Fig. 8 reveals that mixing of primary fassaites with metal (metal B in Fig. 8) that has an elevated $\varepsilon^{182}W$ compared to the $\varepsilon^{182}W$ at the time of CAI formation (metal A in Fig. 8) cannot reproduce the pattern observed in the Hf–W data for CAIs and their constituents. The hypothetical mixture of metal with the melilite-rich separates as well as the fassaite–metal mixture would only plot on a given regression line

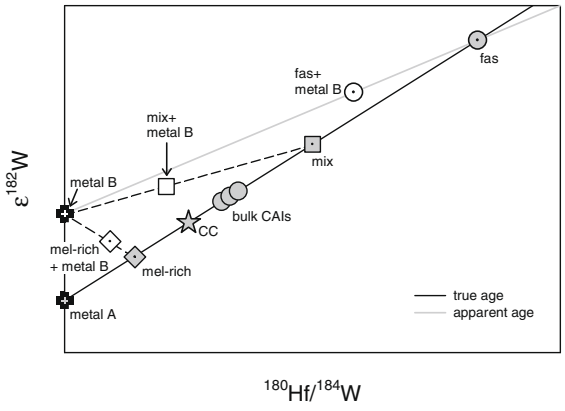

Fig. 8. Illustration showing how mixing of secondary, more radiogenic metal with primary fassaite and melilite could affect the slope of the Hf–W isochron. Note that the illustration is not to scale and that the melilite and mix fractions would not plot on the mixing line between secondary metal and primary fassaite.

if the mixing for each of the fractions fortuitously occurred in the right proportions, which is highly unlikely. Moreover, any such mixing line would pass above the chondritic value and also above the data points for bulk CAIs. However, average carbonaceous chondrites as well as the bulk CAIs investigated here plot on the CAI isochron.

The low MSWD for the A-ZH-6, A-ZH-7 and N-ZH-9 isochrons (MSWD = 0.1–0.52) as well as the fact that all separates (with the exception of A-ZH-8), bulk CAIs and average carbonaceous chondrites plot on a single well-defined isochron (MSWD = 0.56) provides further evidence that the Hf–W systematics in these CAIs were not disturbed by parent body processes. Significant disturbance of the Hf–W systematics should be most pronounced in the Hf–W data for the fines fraction because alteration products will be the most friable among the CAI phases and as a consequence, they should be enriched in the fines fraction. With the exception of A-ZH-8 this is not observed in the Hf–W data of the CAIs investigated here (Fig. 3).

In contrast to the other CAIs, the Hf–W system in A-ZH-8 is slightly disturbed (MSWD = 6.8) and the fines fractions plot above the regression line. Note however that both the initial $\varepsilon^{182}W$ and $^{182}Hf/^{180}Hf$ obtained from the A-ZH-8 isochron, albeit quite imprecise, are consistent with the values obtained from the other isochrons. A-ZH-8 has the highest metal and sulphide content among the CAIs investigated here and fassaites from A-ZH-8 have higher W contents compared to the other analyzed fractions, whereas for all other CAIs the W content in the fassaites is the lowest among the coexisting phases (Fig. 6). This suggests that the disturbance of the Hf–W systematics might have involved redistribution of W during alteration on the parent body.

5.1.3. Significance of the CAI isochron: CAI formation vs. parent body metamorphism

The internal Hf–W isochron for CAIs provides the initial Hf and W isotope compositions at the time of the last isotope equilibration in these CAIs. This refers to the time of cooling below the closure temperature (T_c) of the Hf–W system in CAIs. The CAI isochron, therefore, provides the initial $\varepsilon^{182}W$ and $^{182}Hf/^{180}Hf$ at the time of CAI formation if CAIs cooled below the Hf–W closure temperature shortly after their formation and if later re-heating on the parent body remained at temperatures well below T_c. In their LA-ICPMS study on Hf and W distributions in CAIs, Humayun et al. (2007) state that "OAs [opaque assemblages] adjacent to fassaites are most likely to exchange W isotopically". These authors however do not provide any information regarding the temperatures required for diffusion of W in fassaite but such information is essential for evaluating whether diffusion of radiogenic ^{182}W out of fassaites could have occurred. Depending on the method used, the petrologic type assigned to Allende varies from CV3.2 (Guimon et al., 1995) to CV3.6 (Bonal et al., 2006). Temperature estimates are ~350 °C for aqueous alteration (Krot et al., 1995) and ~400–550 °C for thermal metamorphism (Blum et al., 1989; Weinbruch et al., 1994). The preservation of ^{26}Mg excesses in anorthites in CAIs from CV3 chondrites also requires that heating during parent body metamorphism did not exceed ~500 °C, otherwise Mg diffusion would have erased any pre-existing Mg isotope heterogeneity (LaTourrette and Wasserburg, 1998).

The closure temperature for the Hf–W system in a pyroxene–metal system has been estimated using a numerical model (Van Orman et al., 2001, 2006) and Hf–W ages for H chondrites (Kleine et al., 2008b). These results show that for a wide range in cooling rates and even for grain sizes of pyroxenes of less than 10 μm, the Hf–W closure temperature is essentially identical to the peak metamorphic temperatures of type 6 ordinary chondrites (i.e., ~900–950 °C for H chondrites). Even in H chondrites of petrologic type 4, the Hf–W system has not been reset during thermal metamorphism, in spite of heating up to ~700 °C (Kleine et al., 2008b). Therefore, in contrast to the statement of Humayun et al. (2007), significant diffusion of W in fassaite, the major host of radiogenic ^{182}W in CAIs, could not have taken place during parent body metamorphism of CV3 chondrites because temperatures remained well below T_c for the Hf–W system.

The Hf–W closure temperatures in CAI constituents other than fassaites are less well constrained. The evidence for a late Mg isotopic exchange between anorthite and melilite in some Allende CAIs (Podosek et al., 1991) raises the question as to whether the Hf–W system in the minerals other than fassaites may have been open. Melilite and anorthite do not contain significant amounts of neither Hf nor W but perovskite is an important host of Hf (and probably also W). There are no experimental data available for W diffusion in perovskite but the diffusivity of W can be estimated from diffusion creep data for perovskite. This allows an effective diffusion coefficient to be estimated (Li et al., 1996). This effective diffusion coefficient probably presents Ti and, hence, is a reasonable proxy for W diffusion. At 500 °C the diffusion coefficients are extremely small and diffusion is inefficient even over timescales of billions of years. Another way to assess whether the Hf–W system may have been partially open is to only regress the fassaite and bulk CAI data (this approach assumes that W diffusion across the bulk CAIs was negligible, which seems reasonable for CAIs that are 1 cm across). The regression of the Hf–W data for fassaites from A-ZH-6, -7, and N-ZH-9 and bulk CAIs A-ZH-1 to -4 yields an initial $^{182}Hf/^{180}Hf$ of $(9.7 \pm 0.5) \times 10^{-5}$ and an initial $\varepsilon^{182}W$ of -3.28 ± 0.15, identical to the values obtained from the combined CAI isochron. This and the experimental data for diffusion in perovskite suggest that W diffusion in CAI minerals caused by parent body metamorphism was subdued.

5.1.4. Improved initial Hf and W isotope compositions of CAIs

Given the evidence for undisturbed Hf–W systematics, the Hf–W isochrons for CAIs A-ZH-6, A-ZH-7, and N-ZH-9 provide the initial $\varepsilon^{182}W$ and $^{182}Hf/^{180}Hf$ at the time of Hf–W closure in these CAIs. Since CAIs cooled rapidly (Stolper, 1982), these isochrons provide the $\varepsilon^{182}W$ and $^{182}Hf/^{180}Hf$ at the time of CAI crystallization. All fractions from these CAIs together with the bulk CAIs investigated here (with the exception of A-ZH-5 with its anomalous W isotopic composition) as well as CAIs A37, A44a, and

All-MS-1 plot on a single well-defined isochron (Fig. 4). Average carbonaceous chondrites also plot on this isochron, as expected if carbonaceous chondrites represent the material from which CAIs formed. The regression of all the CAI data (excluding A-ZH-8) yields an initial $^{182}Hf/^{180}Hf = (9.72 \pm 0.44) \times 10^{-5}$ and initial $\varepsilon^{182}W = -3.28 \pm 0.12$ (MSWD = 0.6) (for details see Fig. 4 and Table 4). Using $^{182}W/^{184}W$ ratios normalized to $^{186}W/^{184}W$ (instead of $^{186}W/^{183}W$) yields identical results of $^{182}Hf/^{180}Hf = (9.75 \pm 0.43) \times 10^{-5}$ and initial $\varepsilon^{182}W = -3.21 \pm 0.13$ (MSWD = 1.0). Including the data for A-ZH-8 also does not change the slope and initial $\varepsilon^{182}W$ [$^{182}Hf/^{180}Hf = (9.70 \pm 0.51) \times 10^{-5}$; $\varepsilon^{182}W = -3.26 \pm 0.14$] but results in a higher MSWD (Table 4).

Compared to earlier estimates (Kleine et al., 2002; Yin et al., 2002; Kleine et al., 2005), the initial $^{182}Hf/^{180}Hf$ ratio and $\varepsilon^{182}W$ value determined here are more precise by a factor of almost 2. This results in a substantial increase in the precision of calculated Hf–W ages and potentially allows resolution of time differences as small as ~1 Ma.

5.2. Hf–W systematics of bulk CAIs

The limited spread in Hf/W ratios among the bulk CAIs investigated here precludes the determination of a precise Hf–W isochron for bulk CAIs. Earlier reported Hf–W data for 'bulk' CAIs A44a (Yin et al., 2002) and A37 (Kleine et al., 2005) exhibit a much larger range in Hf/W and $\varepsilon^{182}W$ than is observed for the bulk CAIs investigated here but the A37 and A44a material consists only of the interior of these CAIs and hence is not representative for their bulk chemical composition. Note that A-ZH-2 and A44a are 'bulk' samples of the same CAI. The fractionated Hf/W ratios and variable $\varepsilon^{182}W$ values reported for A37 and A44a are therefore most likely due to sample heterogeneities and are probably caused by a higher proportion of melilite (with low Hf/W and $\varepsilon^{182}W$) in the analyzed fraction of A37 and a higher proportion of fassaite (with high Hf/W and $\varepsilon^{182}W$) in the analyzed fraction of A44a. Most of the bulk CAIs studied here are probably not true bulk CAIs because the entire CAI could not be separated from the Allende host meteorite. The only true bulk CAIs are A-ZH-1 and A-ZH-5, which were located inside the slices, such that the entire material could be processed. It is remarkable that these two CAIs have almost identical $^{180}Hf/^{184}W$ ratios of ~1.83 and ~1.79, whereas CAIs A-ZH-2 to -4 have $^{180}Hf/^{184}W$ ratios below and above these values. This suggests that the slight variability in Hf–W systematics observed among the bulk CAIs investigated here might be due to a slight sampling bias. In this case the Hf/W ratio of bulk CAIs might be best given by CAIs A-ZH-1 and -5.

The slightly elevated $^{180}Hf/^{184}W$ and $\varepsilon^{182}W$ of bulk CAIs compared to the average carbonaceous chondrites value of 1.23 ± 0.08 (Kleine et al., 2004) can be used to constrain the timing and origin of this Hf–W fractionation event. Fegley and Palme (1985) observed depletions of W and Mo relative to other refractory metals (Ir, Os, Ru, etc.) in several CAIs and attributed this depletion to incomplete condensation of W (and Mo) under oxidizing conditions. Other authors however assign these depletions to low-temperature alteration processes on the parent body (Blum et al., 1989). Although no precise Hf–W isochron for bulk CAIs could be obtained here, the Hf–W model age of ~0–3 Myr for bulk CAIs relative to average carbonaceous chondrites suggests that these CAIs acquired their elevated Hf/W ratios in less than ~3 Myr after their formation. As the CV parent body probably accreted later than ~2–3 Myr after CAI formation, as indicated by the youngest ages for CV chondrules (see below), the elevated Hf/W ratios of CAIs are most likely due to nebular processes. The Hf–W systematics of bulk CAIs might therefore reflect loss of W during condensation under oxidizing conditions. In this case these CAIs should also exhibit negative Ce anomalies (Davis et al., 1982), such that determining REE concentrations for these CAIs could constitute an important test for this hypothesis. Although only five CAIs were investigated here it is remarkable that all of them show elevated Hf/W ratios relative to CI chondrites. This might indicate that depletion of W by condensation under high-f_{O_2} conditions is a common feature of CAIs, consistent with earlier observations (Fegley and Palme, 1985). This, however, is inconsistent with evidence from Ti^{3+}/Ti^{4+} ratios in pyroxenes from CAIs that seem to require formation under low-f_{O_2} conditions similar to those of a solar gas (Simon et al., 2007). Clearly, a combined investigation of these redox indicators for a suite of CAIs is needed to investigate under which f_{O_2} conditions CAIs formed.

Table 4
Initial $^{182}Hf/^{180}Hf$ ratios and $\varepsilon^{182}W$ values obtained from CAI isochrons using different normalization schemes.[a]

Sample	Normalization to $^{186}W/^{183}W$			Normalization to $^{186}W/^{184}W$		
	$(^{182}Hf/^{180}Hf)_i \times 10^5 \pm 2\sigma$	$(\varepsilon^{182}W)_i \pm 2\sigma$	MSWD	$(^{182}Hf/^{180}Hf)_i \times 10^5 \pm 2\sigma$	$(\varepsilon^{182}W)_i \pm 2\sigma$	MSWD
A-ZH-6	10.1 ± 0.8	-3.27 ± 0.40	0.1	9.85 ± 0.69	-3.17 ± 0.43	0.1
A-ZH-7	9.17 ± 0.88	-3.21 ± 0.28	0.2	9.71 ± 0.98	-3.27 ± 0.30	1.2
A-ZH-8	10 ± 12	-3.0 ± 2.9	6.8	11 ± 10	-3.4 ± 1.7	7.4
N-ZH-9	9.54 ± 0.90	-3.19 ± 0.32	0.5	9.6 ± 1.0	-3.34 ± 0.37	0.4
Combined CAI isochron	9.70 ± 0.51	-3.26 ± 0.14	1.3	9.78 ± 0.53	-3.20 ± 0.15	1.5
Combined CAI isochron (excl. A-ZH-8)	9.72 ± 0.44	-3.28 ± 0.12	0.6	9.75 ± 0.43	-3.21 ± 0.13	1.0

[a] all regression calculated using the model 1 fit of IsoPlot. Details regarding the regressions are given in Figs. 3 and 4. Note that the regressions for the combined CAI isochron (both with and without A-ZH-8) include previously reported Hf–W data for CAIs (Kleine et al., 2005; Yin et al., 2002).

6. SHORT-LIVED RADIONUCLIDES IN THE EARLY SOLAR SYSTEM AND THE AGE OF CAIS

6.1. Distribution of short-lived radionuclides in the early solar system: ^{26}Al vs. ^{182}Hf

The use of short-lived radionuclides as high-resolution chronometers for the early solar system relies on the assumption that their abundance relative to a stable isotope of the same element was initially homogeneous throughout the solar system. The validity of this assumption, however, has been questioned. Whereas the initial ^{182}Hf/^{180}Hf of the solar system is most likely to be the result of continuous galactic nucleosynthesis (e.g., Wasserburg et al., 1996), some authors proposed that the high initial ^{26}Al/^{27}Al measured in CAIs reflects formation by spallation close to the active early Sun (e.g., Shu et al., 1997; Russell et al., 2001). The homogeneity of short-lived radionuclides in the early solar system can be estimated by comparing their initial abundances in a suite of samples that have formed in different regions of the solar nebula and that have a spread in ages that is comparable to the half-lives of the short-lived nuclides of interest. Suitable samples for such a comparison must have been cooled sufficiently rapid, such that differences in closure temperatures could not have resulted in resolvable age differences among the various chronometers. These conditions are met by angrites and CAIs.

The comparison of initial abundances of short-lived radionuclides in angrites and CAIs can be made for the ^{26}Al–^{26}Mg and ^{182}Hf–^{182}W systems. A similar approach for comparing the ^{182}Hf–^{182}W and ^{53}Mn–^{53}Cr systems cannot be made yet because internal isochrons for both systems are only available for the two angrites Sahara 99555 and D'Orbigny, which have indistinguishable ages, and the ^{53}Mn–^{53}Cr systematics of CAIs are complicated by the presence of nucleosynthetic anomalies and disturbance of the Mn/Cr ratios due to parent body alteration (Birck and Allègre, 1985; Lugmair and Shukolyukov, 1998). In Fig. 9 the initial ^{182}Hf/^{180}Hf and ^{26}Al/^{27}Al ratios of CAIs and angrites D'Orbigny and Sahara 99555 are plotted. In this diagram, samples with identical Hf–W and Al-Mg ages should plot on a straight line, whose slope can be calculated from the ratio of the ^{26}Al and ^{182}Hf half-lives. Fig. 9 reveals that the initial ^{182}Hf/^{180}Hf and ^{26}Al/^{27}Al ratios of CAIs and the angrites D'Orbigny and Sahara 99555 plot on a line whose slope of 0.07 ± 0.01 is within uncertainty identical to the expected slope of $t_{1/2}$ (^{26}Al)/$t_{1/2}$(^{182}Hf) $= 0.080 \pm 0.002$.

Nevertheless, the uncertainty on the initial ^{26}Al/^{27}Al and ^{182}Hf/^{180}Hf ratios would allow some heterogeneity. The expected ^{26}Al/^{27}Al ratio of CAIs can be calculated from the initial ^{26}Al/^{27}Al of D'Orbigny/Sahara 99555 of $(5.1 \pm 0.6) \times 10^{-7}$ (Spivak-Birndorf et al., 2005) by using the nominal half-lives of ^{26}Al and ^{182}Hf and the Hf–W formation interval between D'Orbigny/Sahara 99555 and CAIs of 4.1 ± 0.7 Ma. The calculated initial ^{26}Al/^{27}Al of CAIs is $(2.7 \pm 2.0) \times 10^{-5}$, which is lower than but within uncertainty indistinguishable from the ^{26}Al/^{27}Al measured in CAIs. Clearly the uncertainty on the calculated initial ^{26}Al/^{27}Al of the solar system is too large for determining whether any ^{26}Al in CAIs has been produced locally by irradiation of CAI material close the early active Sun (Shu et al., 1997). The large uncertainty on the calculated initial ^{26}Al/^{27}Al is mainly due to the uncertainty of the initial ^{182}Hf/^{180}Hf of CAIs. Therefore, once Hf–W isochrons of much higher precision are available for CAIs it will be possible to determine whether any ^{26}Al in CAIs has been produced locally by irradiation.

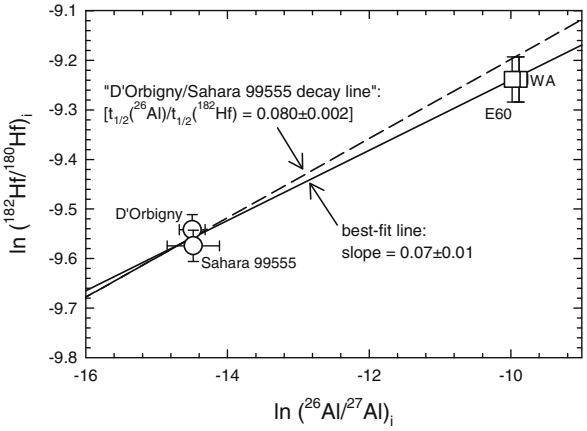

Fig. 9. Measured ^{26}Al/^{27}Al and ^{182}Hf/^{180}Hf ratios for CAIs (E60, WA) and angrites D'Orbigny and Sahara 99555. The solid line is the best-fit line given by the CAI and angrite data and has a slope that is consistent with that expected from the ^{26}Al and ^{182}Hf half-lives. The dashed line is the decay line calculated using the Hf–W and Al-Mg data for D'Orbigny and Sahara 99555 and the ^{182}Hf and ^{26}Al half-lives. Data are from the following references: Al–Mg (Lee et al., 1977; Amelin et al., 2002; Spivak-Birndorf et al., 2005); Hf–W (Kleine et al., 2008a).

A spallogenic origin of some ^{26}Al in CAIs would have a significant impact on the chronology of chondrule formation, which is largely based on Al–Mg chronometry. For instance, if ~50% of the ^{26}Al in CAIs is spallogenic, then the Al–Mg ages for chondrules would be ~1 Myr instead of ~2 Ma. However, as will be shown below (Section 6.3), the overall consistency between Al–Mg and Pb–Pb formation intervals between CAIs and chondrules render it unlikely that CAIs contain significant amounts of spallogenic ^{26}Al but more combined ^{26}Al–^{26}Mg and ^{207}Pb–^{206}Pb on chondrules are needed to confidently establish this.

6.2. Comparison of Hf–W and Pb–Pb ages and the absolute age of CAIs

As for other short-lived isotope systems, differences in initial ^{182}Hf/^{180}Hf ratios only provide relative ages between two meteorites. To convert such relative to absolute ages, knowledge of the ^{182}Hf/^{180}Hf ratio at a well-defined point in time is essential. This approach requires the precise determination of the initial ^{182}Hf/^{180}Hf ratio as well as the absolute age of Hf–W closure in a sample. Due to differences in closure temperatures of different chronometers, the currently best available samples to obtain such information are angrites because (i) they cooled rapidly, such that differences in closure temperatures of the various isotope systems do not result in resolvable age differences, and (ii) they exhibit high U/Pb ratios, such that highly precise ^{207}Pb–^{206}Pb

ages can be obtained (Lugmair and Galer, 1992; Amelin, 2008b; Connelly et al., 2008b).

The comparison of ^{207}Pb–^{206}Pb and Hf–W ages can be made for several angrites including D'Orbigny, Sahara 99555 and Northwest Africa 2999, 4590, and 4801. In Fig. 10 the initial $^{182}Hf/^{180}Hf$ ratios of these angrites are plotted against their ^{207}Pb–^{206}Pb ages. This plot reveals that four of the angrites (D'Orbigny, Sahara 99555, Northwest Africa 4590 and 4801) plot on a straight line, whose slope is identical to the one predicted from the ^{182}Hf half-life. Northwest Africa 2999 plots slightly below but within uncertainty of this line and this probably reflects a slight disturbance of the Hf–W system in this sample (Markowski et al., 2007). An important feature of Fig. 10 is that the calibration of the Hf–W system onto an absolute timescale yields consistent results regardless of which of the four angrites D'Orbigny, Sahara 99555, Northwest Africa 4590 or 4801 is used. This provides evidence that the absolute Hf–W ages calculated relative to these angrites are robust and accurate. By contrast, the absolute Hf–W ages for all of the angrites would be inconsistent with their ^{207}Pb–^{206}Pb ages if the CAI age of 4567.11 ± 0.16 Ma (Amelin et al., 2002; Amelin et al., 2006) were used as an anchor for the Hf–W system (Fig. 10).

The H chondrite Richardton (H5) could in principle also be included in the comparison of ^{207}Pb–^{206}Pb and Hf–W ages but in slowly cooled metamorphic rocks such as H5 chondrites differences in the Hf–W and U-Pb closure temperatures (T_c) could have resulted in age differences. Kleine et al. (2008b) showed that T_c for the Hf–W system in H5 chondrites is 825 ± 75 °C and, hence similar to but slightly above $T_c = 725 \pm 100$ °C for the U-Pb system. Therefore, Hf–W ages should be equal to or older than ^{207}Pb-^{206}Pb ages. It is important to note that, if the absolute Hf–W ages were calculated relative to the ^{207}Pb-^{206}Pb CAI age of 4567.11 ± 0.16 Ma, then the absolute Hf–W age for Richardton would be younger than its ^{207}Pb–^{206}Pb pyroxene age of 4562.7 ± 1.7 Ma (Amelin et al., 2005). This would be inconsistent with the relative diffusivities of W and Pb.

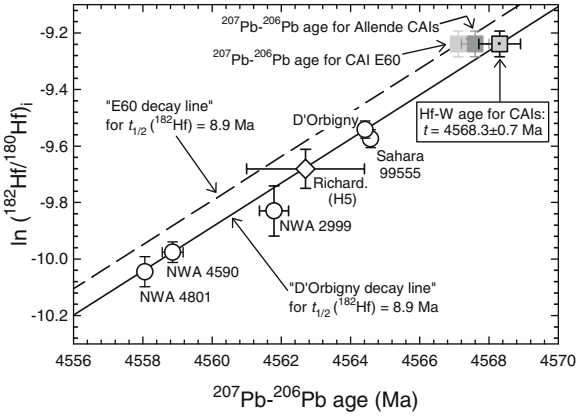

Fig. 10. Measured $^{182}Hf/^{180}Hf$ ratios and ^{207}Pb-^{206}Pb ages in angrites, CAIs and the H5 chondrite Richardton. Data are from the following references: Hf–W data for angrites (Markowski et al., 2007; Kleine et al., 2008a); ^{207}Pb–^{206}Pb ages for angrites (Amelin, 2008b; Connelly et al., 2008b); ^{207}Pb–^{206}Pb age for CAI E60 (Amelin et al., 2002; Amelin et al., 2006); Hf–W data for Richardton (Kleine et al., 2008b); ^{207}Pb–^{206}Pb age for Richardton (Amelin et al., 2005). The $^{182}Hf/^{180}Hf$ for Northwest Africa 2999 is calculated from a pyroxene-metal isochron. Note that angrites plot on a straight line whose slope is consistent with that expected from the ^{182}Hf half-live. Note further that the Hf–W ages of angrites and the H5 chondrite Richardton would be inconsistent with their ^{207}Pb–^{206}Pb ages if the ^{207}Pb–^{206}Pb CAI age of 4567.11 ± 0.16 Ma were used as an age anchor.

The absolute Hf–W ages of CAIs calculated relative to the four angrites D'Orbigny, Sahara 99555, Northwest Africa 4590 or 4801 are summarized in Table 5. Although all of these four absolute Hf–W ages for CAIs are indistinguishable from each other, the Hf–W age calculated relative to Sahara 99555 appears somewhat older than those calculated relative to the other three angrites. This is also evident from the observation that Sahara 99555 plots slightly below but within uncertainty of the "D'Orbigny ^{182}Hf decay line" in Fig. 10 and is consistent with the conclusions of Amelin (2008a) and Connelly et al. (2008b) that the complex U–Pb systematics of Sahara 99555 compromise its use as an absolute time marker for short-lived chronometers. Therefore, the absolute Hf–W age of CAIs is most confidently calculated relative to the three angrites D'Orbigny, NWA 4801 and NWA 4590 and this approach yields an average age of 4568.3 ± 0.7 Ma. The uncertainty on this age results from the uncertainty of the $^{182}Hf/^{180}Hf$ of the CAI isochron (corresponding to an ± 0.6 Myr uncertainty) and the uncertainty introduced by the conversion to absolute ages (which is ± 0.1 Myr as obtained from the standard deviation (2σ) of the absolute Hf–W ages for CAIs calculated relative to these three angrites).

The 4568.3 ± 0.7 Ma Hf–W age for CAIs is consistent with the 4568.5 ± 0.5 Ma Pb–Pb age for CAIs that has been determined from ^{207}Pb–^{206}Pb data for selected fractions of CAIs from Allende and Murchison and Efremovka CAIs E60 and E49 (Bouvier et al., 2007). However, the Hf–W age for CAIs of 4568.3 ± 0.7 Ma is 1.2 ± 0.7 Myr older than the most precise ^{207}Pb–^{206}Pb age for Efremovka CAI E60 of 4567.11 ± 0.16 Ma (Amelin et al., 2006). Taken at face value the Hf–W age for CAIs also is slightly older than the most precise ^{207}Pb–^{206}Pb age for Allende CAIs of

Table 5
Absolute Hf–W age of CAIs as calculated relative to initial $^{182}Hf/^{180}Hf$ ratios and ^{207}Pb-^{206}Pb ages of angrites.[a]

Sample	($^{182}Hf/^{180}Hf$)$_i$ $\times 10^5 \pm 2\sigma$	^{207}Pb-^{206}Pb age	CAI age
Sahara 99555	6.95 ± 0.22	4564.58 ± 0.14	4568.9 ± 0.7
D'Orbigny	7.18 ± 0.22	4564.42 ± 0.12	4568.3 ± 0.7
NWA 4801	4.34 ± 0.23	4558.06 ± 0.15	4568.4 ± 0.9
NWA 4590	4.65 ± 0.17	4558.86 ± 0.30	4568.3 ± 0.8
Average (excl. Sah 99555)			4568.3 ± 0.7

[a] $^{182}Hf/^{180}Hf$ ratios for angrites were recalculated from the data reported in Markowski et al. (2007) and Kleine et al. (2008b) and using the model 1 fit of IsoPlot and $^{180}Hf/^{184}W = 1.18 \times Hf/W$. Pb–Pb ages for angrites are from Amelin (2008b) and Connelly et al. (2008b). Note that the data for Sahara 99555 is not included in the calculated average Hf–W age for CAIs. For details see text.

4567.6 ± 0.4 Ma (Jacobsen et al., 2008) but these two ages agree within their uncertainties. This is also evident from Fig. 10 in which Allende CAIs plot within uncertainty of the "D'Orbigny ^{182}Hf decay line".

An important observation is that while the most precise ^{207}Pb–^{206}Pb ages for Efremovka CAI E60 and Allende CAIs agree with each other, the ^{207}Pb–^{206}Pb age of E60 is different from the Hf–W age for Allende CAIs. The ^{26}Al/^{27}Al of E60 (Amelin et al., 2002) however is identical to those of other CAIs, indicating that E60 formed at the same time than other CAIs (e.g., Lee et al., 1977; Jacobsen et al., 2008). Therefore, the offset between the Hf–W age for CAIs and the ^{207}Pb–^{206}Pb age for E60 requires either that ^{182}Hf was overabundant in CAIs or that the younger ^{207}Pb–^{206}Pb age for E60 does not date the formation of CAIs. Since ^{180}Hf and ^{182}Hf have different *s*- and *r*-process proportions, the first of these options would require that CAIs have *s*- and *r*-process abundances that are different from those of the average solar system (as given for instance by angrites and chondrites). Given that all CAIs except A-ZH-5 have normal *s*- and *r*-process abundances of W isotopes, is seems highly unlikely that the *s*- and *r*-process isotopes of Hf are different from those in average solar system material.

Therefore, the offset between the Hf–W age for Allende CAIs and the ^{207}Pb–^{206}Pb age for E60 seems to imply that the latter does not date CAI formation. The reasons for this are difficult to assess and might be related to a partial resetting of the U–Pb system in CAI E60, while at the same time the Al–Mg and Hf–W systems remained undisturbed. This interpretation is supported by the observation that most CAI samples from Efremovka are not consistent with a single-stage evolution of Pb isotopes (Chen and Papanastassiou, 2008). Efremovka is one of the least altered carbonaceous chondrites but is highly shocked (shock stage S4) and one might speculate that the young ^{207}Pb–^{206}Pb age for E60 reflects the redistribution of volatile Pb during shock. Magnesium and W are much less volatile, such that the effects of shock on the Al–Mg and Hf–W systematics might have been insignificant.

6.3. Consistency of Al-Mg and Pb–Pb ages for chondrules

The Al-Mg system has been the main chronometer used for determining the timescale of chondrule formation (e.g., Russell et al., 1996) but the chronological significance of Al–Mg ages for chondrules has been questioned by some (e.g., Shu et al., 1997; Russell et al., 2001; Gounelle and Russell, 2005). However, the consistency of Al–Mg and ^{207}Pb–^{206}Pb formation intervals between CAIs and chondrules has been an important argument supporting the chronological significance of the Al–Mg chondrule ages (Amelin et al., 2002). It has been customary to use the ^{207}Pb–^{206}Pb CAI age of 4567.11 ± 0.16 Ma as an age anchor for Al-Mg ages, such that the upward revision of the age of CAIs raises the question as to whether the Al–Mg and ^{207}Pb–^{206}Pb formation intervals of chondrules are consistent with a CAI age as old as 4568.3 ± 0.7 Ma.

There are only a few Al–Mg ages available for chondrules from CV and CV-like chondrites and these ages are 2.3 ± 0.6 Myr for chondrules from the CV chondrite Efremovka (Hutcheon et al., 2000), 1.5 ± 0.3 Myr for chondrules from the ungrouped carbonaceous chondrite Acfer 094 (Hutcheon et al., 2000), and 2.1 ± 0.6 and 2.8 ± 0.6 Myr for chondrules from the CV-like chondrite Ningqiang (Hsu et al., 2003). Connelly et al. (2008a) argued that the younger of these ages reflect resetting by parent body processes and that only the oldest of the Al-Mg chondrule ages would reflect chondrule formation. Connelly et al. (2008a) further argue that there is a peak of Al–Mg ages at ~2 Myr after CAI formation, which provides the best estimate for the timing of chondrule formation. This assumption in conjunction with their ^{207}Pb–^{206}Pb age of Allende chondrules of 4565.5 ± 0.5 Ma led Connelly et al. (2008a) to conclude that the age of CAIs could not be older than 4567.5 Ma.

However, the most appropriate data for a comparison of ^{207}Pb–^{206}Pb and Al–Mg ages should come from the same meteorite or at least from the same chondrite group, such that ^{207}Pb–^{206}Pb ages for chondrules for the CV chondrite Allende should be compared with Al–Mg ages for chondrules from the CV chondrite Efremovka or the CV-like chondrite Ningqiang. The ^{207}Pb–^{206}Pb ages for Allende chondrules are 4566.6 ± 1.0 Ma (Amelin and Krot, 2007) and 4565.5 ± 0.5 Ma (Connelly et al., 2008a), which correspond to intervals of 1.7 ± 1.2 Myr and 2.8 ± 0.9 Ma, respectively, relative to the Hf–W age of CAIs of 4568.3 ± 0.7 Ma. The Al–Mg ages for chondrules from CV and CV-like chondrites are 2.1 ± 0.6 and 2.8 ± 0.6 Myr for chondrules from Ningqiang and 2.3 ± 0.6 Myr for chondrules from Efremovka. Within their relatively large uncertainties, the ^{207}Pb–^{206}Pb and Al–Mg intervals are indistinguishable from one another, even for the oldest chondrules from CV and CV-like chondrites. Chondrules from the ungrouped carbonaceous chondrite Acfer 094 appear to be older than the CV chondrules but no ^{207}Pb–^{206}Pb ages are available for the former, rendering a comparison of Al–Mg and ^{207}Pb–^{206}Pb intervals for chondrules from Acfer 094 difficult.

There is a similar consistency between Al–Mg and ^{207}Pb–^{206}Pb ages for chondrules from CR chondrites. Their Al–Mg ages range from ~2 to >4 Myr after CAI formation (Nagashima et al., 2008) and for chondrules from the CR chondrite Acfer 059 ^{207}Pb–^{206}Pb ages of 4564.7 ± 0.6 Ma (Amelin et al., 2002) and 4564.1 ± 0.6 Ma (Connelly et al., 2008a) were reported. These correspond to relative ages of 3.6 ± 0.9 and 4.2 ± 0.9 Myr after CAI formation at 4568.3 ± 0.7 Ma, entirely consistent with the range of Al-Mg ages for CR chondrules. Therefore, currently available Al–Mg and ^{207}Pb–^{206}Pb ages for chondrules from carbonaceous chondrites provide no evidence that CAIs must be younger than 4567.5 Ma and are not inconsistent with an absolute age of CAIs as old as 4568.3 ± 0.7 Ma.

7. FORMATION AND DIFFERENTIATION OF IRON METEORITE PARENT BODIES

7.1. Tungsten model ages for core formation

The W isotope composition of iron meteorites can be used to calculate core formation ages because segregation

of a metal core is accompanied by fractionation of siderophile W from lithophile Hf. The iron core contains no Hf and maintains the $^{182}W/^{184}W$ acquired at the time of its last exchange with the silicate mantle. Hence, the $^{182}W/^{184}W$ of iron meteorites can be used to constrain the time when the metal cores of their parent bodies became completely isolated from the silicate mantle using the following equation (Horan et al., 1998):

$$\Delta t = -\frac{1}{\lambda} \times \ln\left\{\frac{(\varepsilon^{182}W)_{iron} - (\varepsilon^{182}W)_{chondrites}}{(\varepsilon^{182}W)_{CAIs} - (\varepsilon^{182}W)_{chondrites}}\right\} \quad (1)$$

where $\lambda = 0.078 \pm 0.002$ Ma^{-1} (Vockenhuber et al., 2004), $(\varepsilon^{182}W)_{chondrites}$ is the present-day $\varepsilon^{182}W$ of chondrites of -1.9 ± 0.1 (Kleine et al., 2002; Schoenberg et al., 2002; Yin et al., 2002; Kleine et al., 2004), and $(\varepsilon^{182}W)_{CAIs}$ is the initial $\varepsilon^{182}W$ of CAIs as determined in this study. The newly and more precisely defined initial $\varepsilon^{182}W$ of CAIs therefore results in a higher precision of W model ages for iron meteorites.

The calculation of core formation ages is based on several assumptions: (i) iron meteorite parent bodies contained ^{182}Hf, such that their $^{182}W/^{184}W$ could evolve over time; (ii) W isotope equilibration between silicates and metals occurred during core formation; (iii) there are no nucleosynthetic W isotope anomalies in iron meteorites. The available Hf–W data for meteorites suggest that these assumptions are valid. Based on the observation that several differentiated meteorites (including magmatic iron meteorites) exhibit a small deficit in ^{60}Ni, it was suggested that their parent bodies formed prior to the injection of ^{60}Fe that occurred ~1 Myr after CAI formation (Bizzarro et al., 2007). If ^{60}Fe and ^{182}Hf were injected at the same time, then the Ni isotope data of Bizzarro et al. (2007) might be interpreted to imply that magmatic iron meteorites formed prior to injection of ^{182}Hf. However, two more recent studies showed that there are no ^{60}Ni deficits in iron meteorites and argue against a late injection of ^{60}Fe (Dauphas et al., 2008; Regelous et al., 2008). Moreover, a late injection of ^{60}Fe is also inconsistent with the observed Hf–W systematics of meteorites. Although there is no direct evidence for the presence of ^{182}Hf in magmatic iron meteorites (because except for a few silicate-bearing IVA irons they contain no major Hf-bearing phases), most other objects that were inferred by Bizzarro et al. (2007) to have formed in the absence of ^{60}Fe (non-magmatic iron meteorites, angrites, CAIs) have clear evidence for the presence of ^{182}Hf.

It seems unlikely that the unradiogenic $\varepsilon^{182}W$ of magmatic iron meteorites did not equilibrate with silicates during core formation because the temperatures required for core formation were sufficiently high to result in W isotopic exchange between silicates and metal. Segregation of a metal core in small anhydrous asteroids requires that at least ~20% of the solids must have been melted (Taylor, 1992) and that metallic melts could form, indicating temperatures of >1000 °C and probably >1250 °C (Kunihiro et al., 2004). In contrast, the interior of asteroids that remained undifferentiated reached lower temperatures [i.e., ~900–950 °C in the ordinary chondrite (Kessel et al., 2007) and slightly higher temperatures in the acapulcoite/lodranite parent bodies (Zipfel et al., 1995)], causing thermal metamorphism and/or localized melting, respectively. Hafnium–tungsten data for silicates and metals from several ordinary chondrites, acapulcoites and lodranites indicate that the temperatures reached in their parent bodies were sufficient to achieve W isotopic exchange between metal and silicates (Touboul et al., 2007; Kleine et al., 2008b). Consequently, it seems likely that the higher temperatures reached within the parent bodies of the magmatic iron meteorites have a fortiori resulted in the equilibration of W isotopes between metal and silicates.

The presence of nucleosynthetic W anomalies in iron meteorites also cannot account for their unradiogenic $\varepsilon^{182}W$ values. Enrichments or depletions in *s*- or *r*-process components should affect the ^{184}W abundance more strongly than the abundances of the other W isotopes (see Section 4) but no significant ^{184}W anomalies are observed in iron meteorites and the $^{184}W/^{183}W$ ratios of most CAIs, chondrites and iron meteorites are identical at the $\sim \pm 0.2$ ε unit level. Qin et al. (2008a) reported a ~0.1 ε unit deficit in the ^{184}W abundance of IVB irons but these anomalies are too small to affect the $\varepsilon^{182}W$ values significantly.

7.2. Cosmogenic effects in iron meteorites and the chronology of core formation in iron meteorite parent bodies

The chronological interpretation of W isotope data for iron meteorites is complicated by the presence of cosmogenic effects, which are caused by neutron-capture reactions of W isotopes with thermal neutrons produced by the interaction of cosmic rays with meteoritic matter (Masarik, 1997; Leya et al., 2003). These cosmogenic effects result in a decrease of $^{182}W/^{184}W$ of ~0.1 $\varepsilon^{182}W$ per ~100 Ma exposure (Leya et al., 2003; Kleine et al., 2005) but the exact magnitude of these effects strongly depends on the shielding of the samples from cosmic rays (i.e., on the burial depth in the parent bodies), which is difficult to assess. Moreover, the magnitude of the thermal neutron flux that develops in the parent bodies of iron meteorites is difficult to quantify and the moderation of neutrons in a metal matrix is much less effective than in a silicate matrix. In iron meteorite parent bodies, the thermal neutron flux might therefore extend deeper into the parent body.

Most iron meteorites have relatively long exposure times, such that in most cases their $\varepsilon^{182}W$ values were significantly lowered to values more negative than the initial $\varepsilon^{182}W$ of CAIs (Kleine et al., 2005; Markowski et al., 2006b; Schérsten et al., 2006). There is not yet a reliable method to correct for these cosmogenic effects with sufficient precision because no data for nuclides that are sensitive to the thermal neutron flux are available for iron meteorites. Instead, currently employed correction methods rely on the isotopic composition of noble gases and must make assumptions regarding several parameters including the pre-atmospheric size of the meteoroid and the shielding depth of a particular sample (Leya et al., 2003; Markowski et al., 2006a; Qin et al., 2008b). Qin et al. (2008b) applied such a correction method to a range of magmatic iron meteorites and reported corrected $\varepsilon^{182}W$ values ranging from ~−3 to −4. However, given the uncertainties inherent in

these correction methods, the currently most reliable age information regarding core formation in iron meteorite parent bodies is provided by the W isotope composition of magmatic iron meteorites that have young exposure ages or that were large enough for their interior to have been effectively shielded from thermal neutrons. Several authors (Kleine et al., 2005; Lee, 2005; Markowski et al., 2006b) reported W isotope data for the IIAB iron meteorite Negrillos averaging at $\varepsilon^{182}W = -3.42 \pm 0.08$ (2σ). The exposure age of this meteorite is ~50 Ma (Leya et al., 2000) such that the downward shift of $\varepsilon^{182}W$ is only ~0.03 ε (Leya et al., 2003), resulting in a corrected $\varepsilon^{182}W$ of -3.39 ± 0.08 (assuming a 50% uncertainty on the correction). The IVA iron meteorite Gibeon has $\varepsilon^{182}W = -3.38 \pm 0.05$ (Qin et al., 2007) and the low concentrations of cosmogenic noble gases in this meteorite indicate that it is derived from the inner part of a larger body. Therefore, Gibeon was probably more or less completely shielded from thermal neutrons produced by the cosmic rays. Hence, its measured W isotope composition can be interpreted in terms of Hf–W chronometry.

The corrected $\varepsilon^{182}W = -3.39 \pm 0.08$ and measured $\varepsilon^{182}W = -3.38 \pm 0.05$ for Negrillos and Gibeon, respectively, correspond to W model ages for core formation of -1.0 ± 1.3 (2σ) and -0.9 ± 1.2 (2σ) Myr after crystallization of type B CAIs. Relative to the initial $\varepsilon^{182}W$ previously reported in Kleine et al. (2005), these ages were 0.7 ± 1.8 and 0.8 ± 1.7 Myr after CAI formation. Using our newly and more precisely defined initial $\varepsilon^{182}W$ therefore results in W model ages for iron meteorites that are ~0.5 Myr more precise and ~2 Myr older. The uncertainties of these ages were calculated by propagating the uncertainties on the $\varepsilon^{182}W$ values of the iron meteorites, the initial $\varepsilon^{182}W$ of CAIs, and the present-day $\varepsilon^{182}W$ of carbonaceous chondrites. A more conservative approach is to calculate the range of ages obtained from the minimum and maximum $\varepsilon^{182}W$ differences between iron meteorites and CAIs. This approach results in W model ages that range from −2.8 to +0.8 for Negrillos and from −2.5 to +0.6 Myr for Gibeon. Fig. 11 summarizes W model ages for different group of magmatic iron meteorites that are based on $\varepsilon^{182}W$ values that were corrected for cosmic-ray effects using noble gas isotope systematics (Qin et al., 2008b). For the IVB iron meteorites negative ages are obtained, implying that the correction procedure did not fully account for the cosmic-ray effects on their $^{182}W/^{184}W$ ratios. Nevertheless, the range of ages obtained from these corrected $\varepsilon^{182}W$ values is similar to the ages obtained for Negrillos and Gibeon, which have minor to absent cosmic-ray effects. These results imply that core formation in the parent bodies of magmatic iron meteorites occurred within less than ~1 Myr after CAI formation.

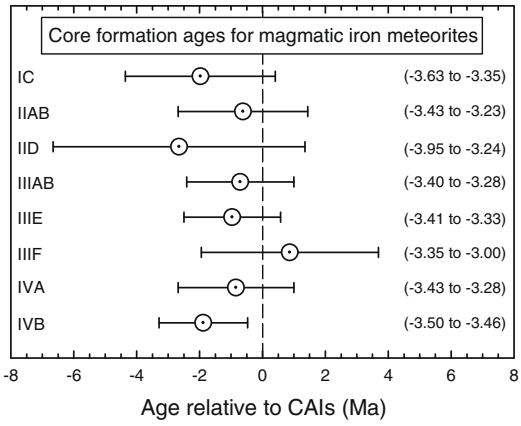

Fig. 11. Tungsten model ages for magmatic iron meteorites, calculated using the range of $\varepsilon^{182}W$ values for several groups of iron meteorites after correction for cosmogenic effects as reported in Qin et al. (2008b) and using an initial $\varepsilon^{182}W$ of CAIs of -3.28 ± 0.12, as determined in the present study. Numbers in parentheses correspond to the range of corrected $\varepsilon^{182}W$ for groups of magmatic iron meteorites. Note that the uncertainties in the W model ages include the uncertainty on the initial $\varepsilon^{182}W$ of CAIs. The IVB irons have corrected $\varepsilon^{182}W$ values that are lower than the initial $\varepsilon^{182}W$ of CAIs, suggesting that the correction procedure employed by Qin et al. (2008b) did not fully correct the cosmic-ray effect on the $^{182}W/^{184}W$ ratio.

8. CONCLUSIONS

The relative ^{183}W, ^{184}W, and ^{186}W abundances of most of the bulk CAIs investigated here are indistinguishable from those of bulk chondrites, eucrites, most iron meteorites, and the terrestrial standard. Only one CAI has a ^{184}W deficit that most likely reflects a higher proportion of *r*-process relative to *s*-process W isotopes. For the first time, precise Hf–W data for pure fassaite separates and fassaite-free fractions from CAIs were obtained. The newly and more precisely defined Hf–W isochron for CAIs provides improved Hf and W isotope compositions at the time of CAI formation and the initial $\varepsilon^{182}W$ of -3.28 ± 0.12 and the initial $^{182}Hf/^{180}Hf$ ratio of $(9.72 \pm 0.44) \times 10^{-5}$ are a factor of ~2 more precise than earlier estimates. Moreover, the initial $\varepsilon^{182}W$ is slightly higher than but within uncertainties identical to an earlier estimate.

Based on the Hf–W isochron for CAIs and Hf–W and U–Pb data for several angrites, the absolute age of CAIs is 4568.3 ± 0.7 Ma. This age is 0.5–2 Myr older than the ^{207}Pb–^{206}Pb age of 4567.11 ± 0.16 Ma for Efremovka CAI E60. The latter, therefore, does not seem to date the formation of CAIs. Contrary to a recent proposal (Connelly et al., 2008a), a CAI age as old as 4568.3 ± 0.7 Ma is entirely consistent with Al–Mg and ^{207}Pb–^{206}Pb ages for chondrules from carbonaceous chondrites.

The Hf–W isochron for CAIs presented here provides a more precisely defined initial $\varepsilon^{182}W$ of CAIs, which in principle allows the timing of core formation in asteroids to be determined with a higher precision. However, the presence of cosmogenic effects and difficulties in reliably quantifying them currently hamper the determination of more precise core formation ages. The increase in $\varepsilon^{182}W$ by ~0.1 in the first Myr after formation of CAIs is of the same order as the expected cosmogenic effects even in iron meteorites with short exposure times or effective shielding from cosmic rays. Hence, even small cosmogenic effects that are essentially undetectable with current analytical techniques can have a significant effect on the calculated ages. In addition, uncer-

tainties in the initial W isotope composition of CAIs that may arise from slight disturbances by parent body processes also limit the precision to which W model ages for iron meteorites can be obtained.

It can nevertheless be stated with confidence that core formation in the parent bodies of magmatic iron meteorites predated chondrule formation at >2 Myr. For instance, the estimated cosmogenic effect on the W isotope composition of Negrillos is ~−0.03 ε, corresponding to an age correction of ~0.3 Myr. Therefore, only if the correction were ~10 times larger would the core formation age be younger than the chondrule ages. It is however unlikely that the correction equations (Leya et al., 2003) are inaccurate by one order of magnitude. Likewise, although parent body processes might have slightly affected the initial W isotope composition of CAIs, the Hf–W data for CAIs presented in this study are difficult to reconcile with an initial $\varepsilon^{182}W$ at the time of CAI formation significantly lower than ~−3.4. However, only if the initial $\varepsilon^{182}W$ of CAIs would be lower than ~−3.7 could the Hf–W timescale for core formation in iron meteorite parent bodies be coeval to chondrule formation. Therefore, the results presented here validate earlier conclusions that the accretion and differentiation of the parent bodies of magmatic iron meteorites predated chondrule formation and, hence, accretion of chondrite parent asteroids (Kleine et al., 2005).

ACKNOWLEDGMENTS

We thank the National Museum of Natural History of the Smithsonian Institution (Washington, DC) for providing the Allende slices. Discussions with Laurence Grossmann, Munir Humayun, Larry Nyquist, and John Wasson were particular useful. Rainer Wieler is thanked for an informal review of our manuscript and Jim Van Orman is thanked for his advice on estimating the diffusion behavior of W in CAIs. We thank Andy Davis for a constructive review and Norika Kita for her comments and editorial efforts, which greatly improved the paper. We also thank Ghylaine Quitté and Qing-Zhu Yin for their critical reviews. This work was supported by a DAAD stipend to Christoph Burkhardt.

REFERENCES

Amelin Y., Krot A. N., Hutcheon I. D. and Ulyanov A. A. (2002) Lead isotopic ages of chondrules and calcium–aluminum-rich inclusions. *Science* **297**, 1678–1683.

Amelin Y., Ghosh A. and Rotenberg E. (2005) Unraveling the evolution of chondrite parent asteroids by precise U–Pb dating and thermal modeling. *Geochim. Cosmochim. Acta* **69**, 505–518.

Amelin Y., Wadhwa M. and Lugmair G. W. (2006) Pb-isotopic dating of meteorites using ^{202}Pb–^{205}Pb double spike: comparison with other high-resolution chronometers. *Lunar Planet. Sci. Conf.* **XXXVII**, abstract no. 1970.

Amelin Y. and Krot A. N. (2007) Pb isotopic ages of the Allende chondrules. *Meteorit. Planet. Sci.* **42**, 1321–1335.

Amelin Y. (2008a) The U–Pb systematics of angrite Sahara 99555. *Geochim. Cosmochim. Acta* **72**, 4874–4885.

Amelin Y. (2008b) U–Pb ages of angrites. *Geochim. Cosmochim. Acta* **72**, 221–232.

Armstrong J. T., Hutcheon I. D. and Wasserburg G. J. (1987) Zelda and Company—petrogenesis of sulfide-rich Fremdlinge and constraints on solar nebula processes. *Geochim. Cosmochim. Acta* **51**, 3155–3173.

Baker J. A., Bizzarro M., Wittig N., Connelly J. and Haack H. (2005) Early planetesimal melting from an age of 4.5662. *Nature* **436**, 1127–1131.

Becker H., Morgan J. W., Walker R. J., MacPherson G. J. and Grossman J. N. (2001) Rhenium–osmium systematics of calcium–aluminium-rich inclusions in carbonaceous chondrites. *Geochim. Cosmochim. Acta* **65**, 3379–3390.

Birck J. L. and Allègre C. J. (1985) Evidence for the presence of ^{53}Mn in the early solar system. *Geophys. Res. Lett.* **12**, 745–748.

Birck J. L. (2004) An overview of isotopic anomalies in extraterrestrial materials and their nucleosynthetic heritage. In *Geochemistry of Non-traditional Stable Isotopes* (eds. C. M. Johnson, B. L. Beard and F. Albarede). The Mineralogical Society of America, Washington, pp. 25–64.

Bischoff A. and Palme H. (1987) Composition and mineralogy of refractory-metal-rich assemblages from a Ca,Al-rich inclusions in the Allende meteorite. *Geochim. Cosmochim. Acta* **51**, 2733–2748.

Bizzarro M., Baker J. A., Haack H. and Lundgaard K. L. (2005) Rapid timescales for accretion and melting of differentiated planetesimals inferred from ^{26}Al–^{26}Mg chronometry. *Astrophys. J.* **632**, L41–L44.

Bizzarro M., Ulfbeck D., Trinquier A., Thrane K., Connelly J. N. and Meyer B. S. (2007) Evidence for a late supernova injection of Fe-60 into the protoplanetary disk. *Science* **316**, 1178–1181.

Blum J. D., Wasserburg G. J., Hutcheon I. D., Beckett J. R. and Stolper E. M. (1989) Origin of opaque assemblages in C3V meteorites—implications for nebular and planetary processes. *Geochim. Cosmochim. Acta* **53**, 543–556.

Bonal L., Quirico E., Bourot-Denise M. and Montagnac G. (2006) Determination of the petrologic type of CV3 chondrites by Raman spectroscopy of included organic matter. *Geochim. Cosmochim. Acta* **70**, 1849–1863.

Bouvier A., Blichert-Toft J., Moynier F., Vervoort J. D. and Albarède F. (2007) Pb–Pb dating constraints on the accretion and cooling history of chondrites. *Geochim. Cosmochim. Acta* **71**, 1583–1604.

Campbell A. J., Simon S. B., Humayun M. and Grossman L. (2003) Chemical evolution of metal in refractory inclusions in CV3 chondrites. *Geochim. Cosmochim. Acta* **67**, 3119–3134.

Chen J. H. and Tilton G. R. (1976) Isotopic lead investigations on Allende carbonaceous chondrite. *Geochim. Cosmochim. Acta* **40**, 635–643.

Chen J. H. and Wasserburg G. J. (1981) The isotopic composition of uranium and lead in Allende inclusions and meteoritic phosphates. *Earth Planet. Sci. Lett.* **52**, 1–15.

Chen J. H. and Papanastassiou D. A. (2008) The concordancy of uranium-lead ages in meteorites. *Lunar Planet. Sci. Conf.* **XXXIX**, abstract no. 1956.

Connelly J., Amelin Y., Krot A. N. and Bizzarro M. (2008a) Chronology of the solar system's oldest solids. *Astrophys. J.* **675**, L121–L124.

Connelly J., Bizzarro M., Thrane K. and Baker J. A. (2008b) The Pb–Pb age of angrite Sah99555 revisited. *Geochim. Cosmochim. Acta* **72**, 4813–4824.

Corgne A. and Wood B. J. (2002) $CaSiO_3$ and $CaTiO_3$ perovskite–melt partitioning of trace elements: Implications for gross mantle differentiation. *Geophys. Res. Lett.* **29**, 4.

Dauphas N., Cook D. L., Sacarabany A., Frohlich C., Davis A. M., Wadhwa M., Pourmand A., Rauscher T. and Gallino R. (2008) Iron-60 Injection in the Protosolar Nebula: how early and how well mixed? *Lunar Planet. Sci. Conf.* **XXXIX**, abstract no. 1170.

Davis A. M., Tanaka T., Grossman L., Lee T. and Wasserburg G. J. (1982) Chemical composition of HAL, an isotopically-unusual Allende inclusion. *Geochim. Cosmochim. Acta* **46**, 1627–1651.

El Goresy A., Nagel K. and RamdohrP. (1978) Fremdlinge and their noble relatives. In *Proc. 9th Lunar Planet. Sci. Conf.*, pp. 1279–1303.

Fegley B. and Palme H. (1985) Evidence for oxidizing conditions in the solar nebula from Mo and W depletions in refractory inclusions in carbonaceous chondrites. *Earth Planet. Sci. Lett.* **72**, 311–326.

Floss C., El Goresy A., Palme H., Spettel B. and Zinner E. (1992) An unusual Ca–Ti–Al silicate in a type-A Allende inclusion. *Meteoritics* **27**, 220.

Friedrich J., Ebel D. S., Weisberg M. K. and Birdsell J. (2005) The crucible: an unusual matrix-enclosing igneous CAI in NWA 2364 (CV3). *Lunar Planet. Sci. Conf.* **XXXVI**, abstract no. 1756.

Fuchs L. H. (1978) The mineralogy of a rhoenite-bearing calcium aluminum rich inclusion in the Allende meteorite. *Meteoritics* **13**, 73–88.

Gounelle M. and Russell S. S. (2005) Spatial heterogeneity of short-lived isotopes in the solar accretion disk and early solar system chronology. In *Chondrites and the protoplanetary disk* (eds. A. N. Krot, E. R. D. Scott and B. Reipurth). Astronomical Society of the Pacific, pp. 588–601.

Gray C. M., Papanastassiou D. A. and Wasserburg G. J. (1973) Identification of early condensates from solar nebula. *Icarus* **20**, 213–239.

Grossman L. (1972) Condensation in the primitive solar nebula. *Geochim. Cosmochim. Acta* **36**, 597–619.

Grossman L. (1975) Petrography and mineral chemistry of Ca-rich inclusions in the Allende meteorite. *Geochim. Cosmochim. Acta* **39**, 433–434, IN1–IN2, 435–454.

Grossman L. (1980) Refractory inclusions in the Allende meteorite. *Annu. Rev. Earth Planet. Sci.* **8**, 559–608.

Guimon R. K., Symes S. J. K., Sears D. W. G. and Benoit P. H. (1995) Chemical and physical studies of type 3 chondrites XII: the metamorphic history of CV chondrites and their components. *Meteoritics* **30**, 704–714.

Horan M. F., Smoliar M. I. and Walker R. J. (1998) ^{182}W and ^{187}Re–^{187}Os systematics of iron meteorites: Chronology for melting, differentiation, and crystallization in asteroids. *Geochim. Cosmochim. Acta* **62**, 545–554.

Horan M. F., Walker R. J., Morgan J. W., Grossman J. N. and Rubin A. E. (2003) Highly siderophile elements in chondrites. *Chem. Geol.* **196**, 5–20.

Hsu W. B., Huss G. R. and Wasserburg G. J. (2003) Al-Mg systematics of CAIs, POI, and ferromagnesian chondrules from Ningqiang. *Meteorit. Planet. Sci.* **38**, 35–48.

Humayun M., Simon S. B. and Grossman L. (2007) Tungsten and hafnium distribution in calcium–aluminum inclusions (CAIs) from Allende and Efremovka. *Geochim. Cosmochim. Acta* **71**, 4609–4627.

Huss G. R., MacPherson G. J., Wasserburg G. J., Russell S. S. and Srinivasan G. (2001) Aluminum-26 in calcium–aluminum-rich inclusions and chondrules from unequilibrated ordinary chondrites. *Meteorit. Planet. Sci.* **36**, 975–997.

Hutcheon I. D., Krot A. N. and Ulyanov A. A. (2000) ^{26}Al in anorthite-rich chondrules in primitive carbonaceous chondrites: evidence chondrules postdate CAI. *Lunar Planet. Sci. Conf.* **XXXI**, abstract no. 1896.

Jacobsen B., Yin Q.-z., Moynier F., Amelin Y., Krot A. N., Nagashima K., Hutcheon I. D. and Palme H. (2008) ^{26}Al–^{26}Mg and^{207}Pb–^{206} Pb systematics of Allende CAIs: canonical solar initial ^{26}Al/^{27}Al ratio reinstated. *Earth Planet. Sci. Lett.*. doi:10.1016/j.epsl.2008.05.003.

Kennedy A. K., Lofgren G. E. and Wasserburg G. J. (1993) An experimental study of trace element partitioning between perovskite, hibonite and melt: equilibrium values. *Lunar Planet. Sci. Conf.* **XXIV**, 793–794.

Kessel R., Beckett J. R. and Stolper E. M. (2007) The thermal history of equilibrated ordinary chondrites and the relationship between textural maturity and temperature. *Geochim. Cosmochim. Acta* **71**, 1855–1881.

Kita N. T., Nagahara H., Togashi S. and Morishita Y. (2000) A short duration of chondrule formation in the solar nebula: evidence from ^{26}Al in Semarkona ferromagnesian chondrules. *Geochim. Cosmochim. Acta* **64**, 3913–3922.

Kleine T., Münker C., Mezger K. and Palme H. (2002) Rapid accretion and early core formation on asteroids and the terrestrial planets from Hf–W chronometry. *Nature* **418**, 952–955.

Kleine T., Mezger K., Münker C., Palme H. and Bischoff A. (2004) ^{182}Hf–^{182}W isotope systematics of chondrites, eucrites, and Martian meteorites: chronology of core formation and mantle differentiation in Vesta and Mars. *Geochim. Cosmochim. Acta* **68**, 2935–2946.

Kleine T., Mezger K., Palme H., Scherer E. and Münker C. (2005) Early core formation in asteroids and late accretion of chondrite parent bodies: Evidence from ^{182}Hf–^{182}W in CAIs, metal-rich chondrites and iron meteorites. *Geochim. Cosmochim. Acta* **69**, 5805–5818.

Kleine T., Bourdon B., Burkhardt C. and Irving A. J. (2008a) Hf–W chronometry of angrites: constraints on the absolute age of CAIs and planetesimals accretion timescales. *Lunar Planet. Sci. Conf.* **XXXIX**, abstract no. 2367.

Kleine T., Touboul M., Van Orman J. A., Bourdon B., Maden C., Mezger K. and Halliday A. (2008b) Hf–W thermochronometry: closure temperature and constraints on the accretion and cooling history of the H chondrite parent body. *Earth Planet. Sci. Lett.* **270**, 106–118.

Kornacki A. S. and Wood J. A. (1985) The identification of Group II inclusions in carbonaceous chondrites by electron probe microanalysis of perovskite. *Earth Planet. Sci. Lett.* **72**, 74–86.

Krot A. N., Scott E. R. D. and Zolensky M. E. (1995) Mineralogical and chemical modification of components in CV3 chondrites: nebular or asteroidal processing? *Meteoritics* **30**, 748–775.

Kunihiro T., Rubin A. E., McKeegan K. D. and Wasson J. T. (2004) Initial ^{26}Al/^{27}Al in carbonaceous-chondrite chondrules: too little^{26} Al to melt asteroids. *Geochim. Cosmochim. Acta* **68**, 2947–2957.

Kurahashi E., Kita N. T., Nagahara H. and Morishita Y. (2008) ^{26}Al–^{26}Mg systematics of chondrules in a primitive CO chondrite. *Geochim. Cosmochim. Acta* **72**, 3865–3882.

LaTourrette T. and Wasserburg G. J. (1998) Mg diffusion in anorthite: implications for the formation of early solar system planetesimals. *Earth Planet. Sci. Lett.* **158**, 91–108.

Lee D. C. (2005) Protracted core formation in asteroids: evidence from high precision W isotopic data. *Earth Planet. Sci. Lett.* **237**, 21–32.

Lee T., Papanastassiou D. A. and Wasserburg G. J. (1977) Al-26 in the early solar system—fossil or fuel. *Astrophys. J.* **211**, L107–L110.

Leya I., Wieler R. and Halliday A. N. (2000) Cosmic-ray production of tungsten isotopes in lunar samples and meteorites and its implications for Hf–W cosmochemistry. *Earth Planet. Sci. Lett.* **175**, 1–12.

Leya I., Wieler R. and Halliday A. N. (2003) The influence of cosmic-ray production on extinct nuclide systems. *Geochim. Cosmochim. Acta* **67**, 529–541.

Li P., Karato S. and Wang Z. C. (1996) High-temperature creep in fine-grained polycrystalline $CaTiO_3$, an analogue material of $(Mg,Fe)SiO_3$ perovskite. *Phys. Earth Planet. Int.* **95**, 19–36.

Ludwig K. (1991). ISOPLOT: *A Plotting and Regression Program for Radiogenic Isotope Data*; version 2.53. U.S.G.S. Open File Report 91-0445.

Lugmair G. W. and Galer S. J. G. (1992) Age and isotopic relationships among the angrites Lewis Cliff 86010 and Angra dos Reis. *Geochim. Cosmochim. Acta* **56**, 1673–1694.

Lugmair G. W. and Shukolyukov A. (1998) Early solar system timescales according to ^{53}Mn–^{53}Cr systematics. *Geochim. Cosmochim. Acta* **62**, 2863–2886.

Lundstrom C. C., Sutton A. L., Chaussidon M., McDonough W. F. and Ash R. D. (2006) Trace element partitioning between type B CAI melts and melilite and spinel: Implications for trace element distribution during CAI formation. *Geochim. Cosmochim. Acta* **70**, 3421–3435.

MacPherson G. J., Wark D. A. and Armstrong J. T. (1988) Primitive material surviving in chondrites: refractory inclusions. In *Meteorites and the Early Solar System* (eds. J. F. Kerridge and M. S. Matthews). University of Arizona Press, Arizona, pp. 46–807.

MacPherson G. J. (2007) Calcium–Aluminum-rich inclusions in chondritic meteorites. In *Treatise on Geochemistry* (eds. H. D. Holland and K. K. Turekian). Pergamon, Oxford, pp. 201–246.

Markowski A., Leya I., Quitté G., Ammon K., Halliday A. N. and Wieler R. (2006a) Correlated helium-3 and tungsten isotopes in iron meteorites: quantitative cosmogenic corrections and planetesimal formation times. *Earth Planet. Sci. Lett.* **250**, 104–115.

Markowski A., Quitté G., Halliday A. N. and Kleine T. (2006b) Tungsten isotopic compositions of iron meteorites: chronological constraints vs cosmogenic effects. *Earth Planet. Sci. Lett.* **242**, 1–15.

Markowski A., Quitté G., Kleine T., Halliday A., Bizzarro M. and Irving A. J. (2007) Hf–W chronometry of angrites and the earliest evolution of planetary bodies. *Earth Planet. Sci. Lett.* **262**, 214–229.

Masarik J. (1997) Contribution of neutron-capture reactions to observed tungsten isotopic ratios. *Earth Planet. Sci. Lett.* **152**, 181–185.

Nagashima K., Huss G. R. and Krot A. N. (2008) ^{26}Al in chondrules from CR carbonaceous chondrites. *Lunar Planet. Sci. Conf.* **XXXIX**, abstract no. 2224.

Nyquist L. E., Reese Y., Wiesmann H., Shih C. Y. and Takeda H. (2003) Fossil ^{26}Al and ^{53}Mn in the Asuka 881394 eucrite: evidence of the earliest crust on asteroid 4 Vesta. *Earth Planet. Sci. Lett.* **214**, 11–25.

Palme H. and Wlotzka F. (1976) A metal particle from a Ca–Al-rich inclusion for the meteorite Allende, and condensation of refractory siderophile elements. *Earth Planet. Sci. Lett.* **33**, 45–60.

Palme H., Hutcheon I. D. and Spettel B. (1994) Composition and origin of refractory-metal-rich assemblages in a Ca,Al-rich Allende inclusion. *Geochim. Cosmochim. Acta* **58**, 495–513.

Podosek F. A., Zinner E. K., Macpherson G. J., Lundberg L. L., Brannon J. C. and Fahey A. J. (1991) Correlated study of initial $^{87}Sr/^{86}Sr$ and Al–Mg isotopic systematics and petrologic properties in a suite of refractory inclusions from the Allende meteorite. *Geochim. Cosmochim. Acta* **55**, 1083–1110.

Qin L. P., Dauphas N., Janney P. E. and Wadhwa M. (2007) Analytical developments for high-precision measurements of W isotopes in iron meteorites. *Anal. Chem.* **79**, 3148–3154.

Qin L. P., Dauphas N., Wadhwa M., Markowski A., Gallino R., Janney P. E. and Bouman C. (2008a) Tungsten nuclear anomalies in planetesimal cores. *Astrophys. J.* **674**, 1234–1241.

Qin L. P., Dauphas N., Wadhwa M., Masarik J. and Janney P. E. (2008b) Rapid accretion and differentiation of iron meteorite parent bodies inferred from ^{182}Hf–^{182}W chronometry and thermal modeling. *Earth Planet. Sci. Lett.*. doi:10.1016/j.epsl.2008.06.018.

Regelous M., Elliott T. and Coath C. D. (2008) Nickel isotope heterogeneity in the early Solar System. *Earth Planet. Sci. Lett.*. doi:10.1016/j.epsl.2008.05.001.

Righter K. and Shearer C. K. (2003) Magmatic fractionation of Hf and W: constraints on the timing of core formation and differentiation in the Moon and Mars. *Geochim. Cosmochim. Acta* **67**, 2497–2507.

Rudraswami N. G. and Goswami J. N. (2007) ^{26}Al in chondrules from unequilibrated L chondrites: onset and duration of chondrule formation in the early solar system. *Earth Planet. Sci. Lett.* **257**, 231–244.

Russell S. S., Srinivasan G., Huss G. R., Wasserburg G. J. and Macpherson G. J. (1996) Evidence for widespread ^{26}Al in the solar nebula and constraints on nebula time scales. *Science* **273**, 757–762.

Russell S. S., Gounelle M. and Hutchison R. (2001) Origin of short-lived radionuclides. *Philos. Trans. Roy. Soc. Lond. A* **359**, 1991–2004.

Schérsten A., Elliott T., Hawkesworth C., Russell S. S. and Masarik J. (2006) Hf–W evidence for rapid differentiation of iron meteorite parent bodies. *Earth Planet. Sci. Lett.* **241**, 530–542.

Schoenberg R., Kamber B. S., Collerson K. D. and Eugster O. (2002) New W-isotope evidence for rapid terrestrial accretion and very early core formation. *Geochim. Cosmochim. Acta* **66**, 3151–3160.

Scott E. R. D. and Wasson J. T. (1975) Classification and properties of iron meteorites. *Rev. Geophys.* **13**, 527–546.

Shannon R. D. (1976) Revised effective ionic radii and systematic studies of interatomic distances in halides and chalcogenides. *Acta Crystall.* **A32**, 751–767.

Shu F. H., Shang H., Glassgold A. E. and Lee T. (1997) X-rays and fluctuating x-winds from protostars. *Science* **277**, 1475–1479.

Simon S. B., Grossman L. and Davis A. M. (1991) Fassaite composition trends during crystallization of Allende Type B refractory inclusion melts. *Geochim. Cosmochim. Acta* **55**, 2635–2655.

Simon S. B., Kuehner S. M., Davis A. M., Grossman L., Johnson M. L. and Burnett D. S. (1994) Experimental studies of trace element partitioning in Ca,Al-rich compositions: anorthite and perovskite. *Geochim. Cosmochim. Acta* **58**, 1507–1523.

Simon S. B., Sutton S. R. and Grossman L. (2007) Valence of titanium and vanadium in pyroxene in refractory inclusion interiors and rims. *Geochim. Cosmochim. Acta* **71**, 3098–3118.

Spivak-Birndorf L., Wadhwa M. and Janney P. E. (2005) ^{26}Al–^{26}Mg chronology of the D'Orbigny and Sahara 99555 angrites. *Meteorit. Planet. Sci.* **40,** abstract No. 5097.

Stolper E. (1982) Crystallization sequences from Ca–Al-rich inclusions from Allende: an experimental study. *Geochim. Cosmochim. Acta* **46**, 2159–2180.

Sylvester P. J., Ward B. J., Grossman L. and Hutcheon I. D. (1990) Chemical compositions of siderophile element-rich opaque assemblages in an Allende inclusion. *Geochim. Cosmochim. Acta* **54**, 3491–3508.

Tatsumoto M., Unruh D. M. and Desborough G. A. (1976) U–Th–Pb and Rb–Sr systematics of Allende and U–Th–Pb systematics of Orgueil. *Geochim. Cosmochim. Acta* **40**, 617–634.

Taylor G. J. (1992) Core formation in asteroids. *J. Geophys. Res. Planets* **97**, 14717–14726.

Touboul M., Kleine T., Bourdon B., Zipfel J. and Irving A. J. (2007) Hf–W evidence for rapid accretion and fast cooling of the acapulcoite parent body. *Lunar Planet. Sci. Conf.* **XXXVIII**, abstract no. 2317.

Van Orman J. A., Grove T. L. and Shimizu N. (2001) Rare earth element diffusion in diopside: influence of temperature, pressure and ionic radius, and an elastic model for diffusion in silicates. *Contrib. Mineral. Petrol.* **141**, 687–703.

Van Orman J. A., Saal A. E., Bourdon B. and Hauri E. H. (2006) Diffusive fractionation of U-series radionuclides during mantle melting and shallow level melt–cumulate interaction. *Geochim. Cosmochim. Acta* **70**, 4797–4812.

Vockenhuber C., Oberli F., Bichler M., Ahmad I., Quitté G., Meier M., Halliday A. N., Lee D. C., Kutschera W., Steier P., Gehrke R. J. and Helmer R. G. (2004) New half-life measurement of ^{182}Hf: improved chronometer for the early solar system. *Phys. Rev. Lett.* **93**, art. no. 172501.

Walker R. J., Horan M. F., Morgan J. W., Becker H., Grossman J. N. and Rubin A. E. (2002) Comparative Re-187–Os-187 systematics of chondrites: implications regarding early solar system processes. *Geochim. Cosmochim. Acta* **66**, 4187–4201.

Wasserburg G. J., Busso M. and Gallino R. (1996) Abundances of actinides and short-lived nonactinides in the interstellar medium: diverse supernova sources for the r-processes. *Astrophys. J.* **466**, L109–L113.

Weinbruch S., Armstrong J. T. and Palme H. (1994) Constraints on the thermal history of the Allende parent body as derived from olivine–spinel thermometry and Fe/Mg interdiffusion in olivine. *Geochim. Cosmochim. Acta* **58**, 1019–1030.

Yin Q. Z., Jacobsen S. B., Yamashita K., Blichert-Toft J., Télouk P. and Albarède F. (2002) A short timescale for terrestrial planet formation from Hf–W chronometry of meteorites. *Nature* **418**, 949–952.

Zipfel J., Palme H., Kennedy A. K. and Hutcheon I. D. (1995) Chemical composition and origin of the Acapulco meteorite. *Geochim. Cosmochim. Acta* **59**, 3607–3627.

Associate editor: Noriko Kita